2009

FRAMEWORK ESTABLISHMENT OF TRANSGENIC PLANTAE FACILITATING SYSTEMIC DELIVERY OF GLUCAGON-LIKE PEPTIDE-1 (GLP-1)

Martin E. Brandsma

FRAMEWORK ESTABLISHMENT OF TRANSGENIC PLANTAE FACILITATING SYSTEMIC DELIVERY OF GLUCAGON-LIKE PEPTIDE-1 (GLP-1)

(Spine Title: Expression of GLP-1 and Transferrin in Transgenic Plants)

(Thesis Format: Integrated-Article)

by

Martin E. Brandsma

Graduate Program in Biology

Submitted in partial fulfillment of the
requirements for the degree of
Master of Science

School of Graduate and Postdoctoral Studies
The University of Western Ontario
London, Ontario, Canada

April 2009

ABSTRACT

Human serum transferrin (hsTf) is well characterized for its ability to transport fused therapeutics throughout the body upon oral administration. Glucagon-like peptide-1 (GLP-1) is one such therapeutic, effective against Type II diabetes that could benefit from such a fusion strategy. However, therapeutic use of hsTf and GLP-1 is limited by their generation using current recombinant protein production platforms. This project assesses the viability of accumulating hsTf and GLP-1 independently in transgenic plants as a novel source for the generation of both recombinant proteins. Here, nuclear-transformed tobacco plants stably accumulating either hsTf or a synthetic GLP-1 decamer have been developed. Plant-derived hsTf was shown to reversibly bind iron *in vitro* and the biological activity of GLP-1 was confirmed by its ability to stimulate insulin secretion from a pancreatic cell-line *in vitro*. Overall, results warrant future hsTf-GLP-1 genetic fusions in transgenic plants intended for enhanced bioavailability of GLP-1 upon oral administration.

Key Words: transgenic tobacco, human serum transferrin, human glucagon-like peptide-1, oral administration, recombinant therapeutic proteins, *Agrobacterium*-mediated transformation, nuclear transformation, Type II diabetes mellitus

CO-AUTHORSHIP STATEMENT

The contents of this thesis are part of two manuscripts being prepared to submit for publication. In each of the manuscripts, Martin Brandsma is the primary author, responsible for all experimental design, data collection, interpretation of results as well as writing of the manuscripts. Drs. Anthony Jevnikar and Susanne Kohalmi are presented as co-authors for this research as each contributed to experimental design and defining of the research problem in both manuscripts. Dr. Xiaofeng Wang is also listed as a co-author for each manuscript for his support in data collection. Hong Diao provided support and assistance for all work involving mammalian cell culture. The following two manuscripts are in preparation to submit for publication:

An innovative approach for the assembly of multi-use human serum transferrin
M.E. Brandsma, X. Wang, H. Diao, S.E. Kohalmi, A.M. Jevnikar and S. Ma

A proficient approach to the production of therapeutic glucagon-like peptide-1 (GLP-1) in transgenic plants
M.E. Brandsma, X. Wang, H. Diao, S.E. Kohalmi, A.M. Jevnikar and S. Ma

ACKNOWLEDGEMENTS

I thank my supervisor, Dr. Shengwu Ma for his constant support in the completion of this thesis. This was both a challenging and rewarding process and his continued enthusiasm for science was inspiring. I thank my co-supervisor Dr. Susanne Kohalmi for her insightful feedback and great attention to detail. I would also like to thank the members of my advisory committee Drs. Vojislava Grbic and Norm Hüner for their challenging questions during this process and guidance throughout my entire scientific education.

This work could not have been completed without the members of Dr. Ma's laboratory: Xiaofeng, Reynald, Mike and Hong. Your patience with my many questions and your advice, often much unrelated to science, is seriously valued.

I would like to thank greatly my family who have not had a clue what I've been doing this whole time, but without your love this could not have been possible. Thanks to Andrew Lockey, you are a true friend. Lastly, thanks to Andrea Pitts, my partner in crime, your reassurance and support have made this thesis possible.

TABLE OF CONTENTS

LIST OF TABLES

LIST OF FIGURES

LIST OF ABBREVIATIONS

%	Percent
°C	Degree Celsius
BA	Benzylaminopurine
BHK	Baby hamster kidney
bp	Base pair
BSA	Bovine serum albumin
CaMV	Cauliflower mosaic virus
cDNA	Complementary DNA
cm	Centimetre
ddH_20	Double distilled water
DMEM	Dulbecco's modified eagle media
DNA	Deoxyribonucleic acid
dNTPs	Deoxyribonucleotide triphosphate
DTT	Dithiothreitol
ECL	Enhanced chemiluminescence
EDTA	Ethylene diamine tetra-acetate
ELISA	Enzyme-Linked ImmunoSorbent Assay
g	Grams
G	Gravitational constant (6.67×10^{-11} $m^3/kg/s^2$)
gDNA	Genomic DNA
GI	Gastrointestinal
GTE	Glucose/Tris-HCL/EDTA
h	Hours
IgG	Immunoglobulin G
IMAC	Immobilized metal affinity chromatography
IR	Ischemia reperfusion
kb	Kilobase pair
kDa	Kilo Dalton
kg	Kilogram

kV	Kilovolt
L	Litre
LB	Luria-Bertani media
m	Metre
μg	Microgram
μL	Microlitre
μM	Micromolar
min	Minutes
mg	Milligram
mL	Millilitre
mm	Millimetre
mM	Millimolar
mRNA	Messenger RNA
M	Molar
MSO	Murashige and Skoog salt
NA	Naphthaleneacetic acid
ng	Nanogram
OD	Optical density
PAGE	Polyacrylamide gel electrophoresis
PBS	Phosphate buffer saline
PBST	Phosphate buffer saline with Tween-20
PCR	Polymerase chain reaction
pDNA	Plasmid DNA
PMSF	Phenyl-methylsulfonyl fluoride
PNGaseF	Peptide N-glycosidase F
PVDF	Polyvinylidene difluoride
RNA	Ribonucleic acid
rpm	Revolutions per minute
RTP	Recombinant therapeutic protein
RT-PCR	Reverse transcriptase polymerase chain reaction
s	Seconds

SDS	Sodium dodecyl sulphate
siRNA	Small interfering RNA
TB	Terrific broth
TBS	Tris buffered saline
TBST	Tris buffered saline with Tween-20
TEMED	N,N,N',N'-tetramethylethylmenediamine
TEV	Tobacco etch virus
TMB	3, 3', 5, 5'-tetramethylbenzidine
Tris	2-amino-2-hydroxylmethyl-1, 3-propandiol
TSP	Total soluble protein
TYC	Tryptone/yeast extract/calcium chloride
U	Units
USD	United States dollar
UTL	Untranslated leader sequence
UTR	Untranslated region
UV	Ultraviolet
v/v	Volume per volume
w/v	Weight per volume

Chapter 1

General Introduction

1.1 Problem statement

Recent attention has been directed to the use of therapeutic proteins for the treatment of human disease. Glucagon-like peptide-1 (GLP-1) is one such therapeutic shown to be effective against symptoms associated with Type II diabetes. Though GLP-1 therapy for Type II diabetes is promising, treatment will be limited by current production systems. Furthermore, current therapeutic use of GLP-1 is administered through subcutaneous injection, often causing complications and reduced patient compliance. To alleviate concerns associated with therapeutic injections, oral GLP-1 administration has been proposed. However, oral administration of GLP-1 presents its own inherent obstacles such as degradation of the therapeutic and reduced protein permeability within the gastrointestinal (GI) tract. Endogenous human serum transferrin (hsTf) is capable of acting as a transport chaperone when fused to a therapeutic of interest, safely transporting the therapeutic out of the GI tract and into systemic circulation following oral administration. Future GLP-1 genetic fusions to hsTf may therefore alleviate obstacles associated with oral administration. The purposes of this thesis were to (1) manufacture a novel plant-based bioreactor capable of generating biologically active recombinant (r)GLP-1 and (2), establish the framework for future GLP-1-hsTf genetic fusions in the plant bioreactor by demonstrating plant production of recombinant (r)hsTf viable.

Transgenic plants stably accumulating either rGLP-1 or rhsTf were generated by *Agrobacterium*-mediated nuclear gene transfer and validated for incorporation of the recombinant gene, transcript and protein of interest by PCR, RT-PCR and immunoblotting respectively. Plant-derived rGLP-1 was shown to be biologically active by its ability to stimulate insulin secretion from a mouse pancreatic beta-cell line (MIN6) *in vitro*. Plant-derived rhsTf was shown to retain native biological function by reversibly binding iron *in vitro*.

1.2 Scientific justification

1.2.1 Biological production of therapeutic proteins

Recombinant therapeutic proteins (RTPs) are projected to represent a US$53 billion market by 2010 (Pavlou and Reichert, 2004). Novel RTP production strategies must be implemented to meet growing demand while remaining economically feasible. Current commercially available RTPs are most often generated by mammalian cell culture (57%) or *Escherichia coli* and yeast fermentation (43%), though these bioreactors contain inherent production limitations (Boehm, 2007). Prokaryotic fermentation is unable to process many complex eukaryotic protein motifs. Moreover, many bacterial-generated RTPs accumulate within inclusion bodies, necessitating further purification and subsequently, enhanced production costs (Smith, 2007). The eukaryotic yeast bioreactor is able to produce more exotic RTP motifs, but often RTP product is secreted into the surrounding medium and lost due to degradation (Boehm, 2007). Hyperglycosylation of yeast-derived RTPs is also a concern, as extensive mannose chains are able to reduce RTP potency (Gellissen *et al.*, 1992). Mammalian cell cultures offer

relatively large RTP yield (1 to 3 g/L), but are expensive to maintain (300 to 10,000 USD/g) with viral and oncogenic RTP contamination a realistic concern (Boehm, 2007). Large quantity generation of RTPs for commercial use will certainly be limited by current production strategies. One such therapeutic protein facing potential production limitations is the GLP-1 peptide.

1.2.2 Therapeutic GLP-1 peptide and its production limitations

GLP-1 is an incretin hormone, produced by intestinal endocrine L cells within the body (Holst and Gromada, 2004). Due to its native pleiotropic capabilities, much attention has been given to GLP-1 as a potential therapeutic to combat Type II diabetes and its associated symptoms (Holst, 2007). In both rats and mice, GLP-1 is able to reverse pancreatic beta-cell damage often associated with the onset of Type II diabetes (Bulotta *et al.*, 2004). Therapeutic GLP-1 treatment also decreases glucose levels, stimulates insulin secretion and insulin sensitivity, decreases glucagon secretion, promotes weight loss, delays gastric emptying and limits food intake (appetite suppression) in both humans and animals (Drucker, 2003; Edwards, 2005; Nauck *et al.*, 1993). Much interest is now being focused on how to economically produce vast amounts of GLP-1 for effective treatment against Type II diabetes and its associated symptoms.

Though chemical synthesis is most commonly used for generation of small peptides such as GLP-1 (Kimmerlin and Seebach, 2005), this method is often expensive, producing low yields of active peptide product. Recombinant DNA technology offers the possibility of producing these peptides inexpensively and in large quantities. Intrinsic to

the production of recombinant proteins in all bioreactors, are complications associated with small peptide generation due to recombinant protein degradation and instability. To this end, no bioreactor described to date is capable of producing peptides in similar size to GLP-1 (~3.4 kDa) in commercial quantities. To alleviate this problem, rGLP-1 has been produced in both yeast and *E. coli* as genetically fused tandem repeats to itself, generating an overall larger recombinant protein with enhanced stability (Hou *et al.*, 2007a, b). While rGLP-1 multimer production in microbial systems is viable, cell culture-based systems are still limited by reduced production scalability and an inherent need for sophisticated fermentation facilities, requiring substantial capital investment. In addition, rGLP-1 generated in cell culture-based systems requires extensive purification prior to its use to remove host proteins and potentially harmful compounds such as bacterial endotoxins. Therefore, a novel strategy for the production of biologically active rGLP-1 necessitates further investigation.

1.2.3 Benefits of plant-based bioreactors for RTP production

Transgenic plants have become an attractive alternative to cell and microbial-based bioreactors for the generation of RTPs (Boehm, 2007; Daniell, 2006; Schillberg *et al.*, 2005). Plant-based RTP bioreactors permit unlimited scalability, reduced risk of RTP contamination by mammalian pathogens, as well as lower production costs compared to microbial or mammalian cell-based RTP production systems (Boehm, 2007; Wang *et al.*, 2008). Eukaryotic plants also permit the modification and processing of many transgenic mammalian RTPs. Genetically modified plants contain the capacity to produce recombinant proteins in larger quantities compared

to those produced using mammalian cell-based systems (Daniell *et al.*, 2001). Lastly, transgenic plants accumulating RTPs are able to facilitate oral administration of the RTP(s) of interest by simple consumption of plant material (Ma *et al.*, 2005). This ability eliminates the need to purify RTPs after generation, greatly reducing production costs as well as alleviating concerns often associated with subcutaneous injection such as patient compliance.

To date, a variety of plants have shown viable expression and accumulation of proteins intended for therapeutic use including tobacco, alfalfa, wheat, potato, tomato, corn and soybean (Bardor *et al.*, 2003; Brereton *et al.*, 2007; Cho *et al.*, 2004; Ma *et al.*, 1997; Sandhu *et al.*, 2000; Zeitlin *et al.*, 1998; Zhong *et al.*, 2007). More specifically, tobacco has proven extremely promising as an attractive host for RTP production by offering a number of unique advantages. Farming of tobacco is conducted throughout the world as the plant grows quickly, produces a vast amount of biomass and is easy to harvest, often allowing for multiple harvests of a single plant. Since tobacco is not a food or animal feed crop, it reduces the chance of contaminating natural food chains with transgenic material and recombinant proteins. Furthermore, tobacco has been well researched in the laboratory, often called the "white mouse" of the plant kingdom (Cramer *et al.*, 1996). Methods for transforming tobacco are well documented and are a major reason why tobacco has been extensively used as a production platform for recombinant proteins. Furthermore, tobacco lines have been generated as low-nicotine and low-alkaloid cultivars such as "81V9," allowing plant tissue to be used directly for oral delivery without toxic effects (Ma *et al.*, 1997; Menassa *et al.*, 2007).

1.2.4 Plant-derived rGLP-1

The accumulation of rGLP-1 has been reported in transgenic rice either fused to a protein chaperone or as a pentamer repeat (Sugita *et al.*, 2005; Yasuda *et al.*, 2005, 2006). Originally, no rGLP-1 protein was detected in rice seeds when rGLP-1 was expressed as a monomer fused to the signal peptide of glutelin (a rice storage protein), possibly due to small interfering RNA (siRNA) mediated gene silencing and/or peptide instability and proteolytic degradation (Yasuda *et al.*, 2005). Subsequently, accumulation of rGLP-1 was demonstrated in rice seeds when it was expressed as a fusion protein with globulin (another rice seed storage protein) (Sugita *et al.*, 2005). However, biological activity of the globulin-GLP-1 fusion protein was demonstrated only after physical release of GLP-1 from the fusion protein by *in vitro* enzymatic digestion. Recently, rGLP-1 was shown to accumulate in rice seed when expressed as a pentamer repeat fused to the signal peptide of rice glutelin or the signal peptide of rice chitinase, though biological activity was not demonstrated (Yasuda *et al.*, 2006). While results are promising for plant-based production of rGLP-1, an effective strategy for biologically active rGLP-1 production in plants has yet to be demonstrated. Furthermore, if plant-based production of rGLP-1 is to facilitate oral GLP-1 administration by simple consumption of transgenic plant material, a novel strategy to surmount obstacles associated with oral administration must be investigated.

1.2.5 Oral administration of RTPs

Oral administration of therapeutic proteins has significant advantages over traditional systemic injection including an increase in effectiveness, reduced

complications such as local hypertrophy and an overwhelming patient preference when compared to subcutaneous injection (Hamman *et al.*, 2005; Singh *et al.*, 2008). However, delivery of therapeutic proteins by oral administration does have major inherent obstacles. Orally administered RTPs face poor stability within the GI tract as well as a low level of intestinal permeability due to the physical size of RTPs (Saffran *et al.*, 1997; Singh *et al.*, 2008). Many pharmaceutical strategies have been proposed to enhance RTP bioavailability upon oral administration including incorporation of cell-penetrating peptides (Trehin and Merkle, 2004; Zorko and Langel, 2005), use of transporters and efflux mechanisms (Han and Amidon, 2000; Varma *et al.*, 2003) and absorption enhancers (Salamat-Miller and Johnston, 2005; Ward *et al.*, 2000), although most mechanisms are still somewhat limited by absorptive efficiency. Methods that fuse a protein capable of undergoing *in vivo* receptor-mediated endocytosis to a therapeutic of interest have shown effective transport of therapeutics out of the GI tract (Daugherty and Mrsny, 1999; Hwa Kim *et al.*, 2005; Lim and Shen, 2005; Russell-Jones, 2004). Some results indicate this fusion strategy generates a therapeutic protein even more potent than when administered through subcutaneous injection (Bai *et al.*, 2005). The hsTf protein is one such chaperone capable of transporting fused therapeutics across the GI tract and into systemic circulation upon oral administration (Li and Qian, 2002).

1.2.6 hsTf applications and production

The hsTf protein belongs to a diverse class of beta-1-globulin proteins characterized by an innate ability to reversibly sequester metal ions, playing a vital role in cellular iron absorption and the maintenance of iron homeostasis within the body

(Huebers and Finch, 1987). Independently, there exist multiple therapeutic applications of hsTf including prevention of atransferrinemia (Beutler *et al.*, 2000; Hayashi *et al.*, 1993), eliciting cytoprotective effects against irradiation (Lesnikov *et al.*, 2001), and reducing the onset of ischemia reperfusion (IR) injury (de Vries *et al.*, 2004; Kaminski *et al.*, 2002). Human serum Tf also has many commercial applications, including use in mammalian cell growth media (Barnes and Sato, 1980) and as a bacteriostatic agent (Bullen *et al.*, 1978; Bullen, 1981; Ellison *et al.*, 1988). More importantly, hsTf is capable of acting as an effective delivery chaperone, permitting transcellular therapeutic absorption following oral administration when fused to a therapeutic of interest (Li and Qian, 2002). Indeed, therapeutic granulocyte colony-stimulating factor (GCS-F) genetically linked to hsTf could cross monolayers of cells *in vitro* and elicit a therapeutic effect when administered orally to BDF1 mice (Bai *et al.*, 2005; Widera *et al.*, 2003, 2004). Insulin has also been genetically fused to hsTf to achieve transfer across cell layers *in vitro* and induction of hypoglycaemia when administered orally to rat models of diabetes (Shah and Shen, 1996; Xia *et al.*, 2000). These results make hsTf an ideal chaperone candidate for the transfer of GLP-1 into circulation upon oral administration of transgenic plant material. However, before this fusion strategy can be investigated further, hsTf must be demonstrated capable to accumulate within the plant bioreactor independently. There may indeed be many more benefits to the production of hsTf within plants independent of possible genetic fusions to GLP-1.

Initial attempts at rhsTf production in both yeast and *E. coli* bioreactors proved unsuccessful (Funk *et al.*, 1990; Steinlein *et al.*, 1995). Complications associated with rhsTf production were attributed to the physical size of the recombinant protein

(~76 kDa) as well as its intramolecular complexity, containing 38 internal cysteine residues all involved in internal disulfide bonding (MacGillivray *et al.*, 1998). Furthermore, production of rhsTf in *E. coli* results in rhsTf accumulation within inclusion bodies, designating the recombinant protein useless without extensive purification (Ikeda *et al.*, 1992). To alleviate these production concerns, Mason *et al.*, (2001) demonstrated the ability to accumulate rhsTf in baby hamster kidney (BHK) cells. Though rhsTf accumulation in BHK cells is promising, it is limited by low product yield as well as elevated manufacturing costs (Mason *et al.*, 1993). Due to benefits described above, plant-based generation of rhsTf may prove an appropriate strategy for efficient and cost effective rhsTf production.

1.3 Hypothesis and research questions

The purpose of this thesis is to investigate a novel plant-based production strategy for the generation of rGLP-1 and rhsTf. It is hypothesized transgenic tobacco will be capable of independently accumulating rGLP-1 and rhsTf following subsequent transformation with synthetically designed expression vectors. Furthermore, plant-derived rGLP-1 and rhsTf are hypothesized to retain native biological function. To test the hypothesis, the following four questions are asked:

(1) Is tobacco transformed with *GLP-1* capable of accumulating rGLP-1?

Currently, GLP-1 has not been demonstrated to accumulate in transgenic tobacco as a synthetic decamer repeat. Previous literature describes rGLP-1 accumulation in transgenic rice as a fusion to seed coat proteins as well as a

pentamer repeat. Literature also describes rGLP-1 production in both yeast and *E. coli* in a synthetic multimer configuration. To answer this question, *Agrobacterium*-mediated nuclear gene transfer with an expression vector designed for the constitutive expression of a synthetic *GLP-1* decamer repeat was used to stably transform tobacco plants. Transformed tobacco-leaf material was analyzed for *GLP-1* genome integration, *GLP-1* transcript accumulation and the presence of rGLP-1 protein. It was expected rGLP-1 could accumulate as a synthetic decamer to detectable levels in transgenic tobacco plants.

(2) Is tobacco-derived rGLP-1 biologically active *in vitro*?

To date, only native GLP-1 monomer has been shown capable to stimulate *in vitro* insulin secretion of a mouse pancreatic beta-cell line. To reduce production cost and increase production efficiency, plant-derived rGLP-1 decamer was assessed for its ability to induce *in vitro* insulin secretion in a mouse pancreatic beta-cell line. It was expected tobacco-derived rGLP-1 decamer could retain native biological function *in vitro* without disassociation to its native monomer constituents.

(3) Is tobacco transformed with *hsTf* capable of accumulating rhsTf?

Currently, no reported literature demonstrates the ability of transgenic plants to accumulate rhsTf. The accumulation of rhsTf in traditional microbial cell-based systems has been reported. To answer this question, *Agrobacterium*-mediated nuclear gene transfer with an expression vector

designed for the constitutive expression of *hsTf* was used to stably transform tobacco plants. Transformed tobacco-leaf material was analyzed for *hsTf* genome integration, *hsTf* transcript accumulation and the presence of rhsTf protein. It was expected rhsTf could accumulate to detectable levels in transgenic tobacco plants.

(4) Does tobacco-derived rhsTf retain biological function *in vitro*?

Previous microbial and cell-based expression systems were able to demonstrate the ability of rhsTf to reversibly bind iron *in vitro*. To answer this question, plant-derived rhsTf was assessed by spectrophotometry to determine if it retained its native ability to reversibly bind iron *in vitro*. This capability was further assessed by the ability of plant-derived rhsTf to stimulate mammalian cell growth *in vitro* as well as delay bacteria growth *in vitro*. It was expected plant-derived rhsTf could retain the native biological function of reversibly binding iron *in vitro*.

1.5 References

Bai, Y., Ann, D.K., and Shen, W.C. (2005). Recombinant granulocyte colony-stimulating factor-transferrin fusion protein as an oral myelopoietic agent. Proc. Natl. Acad. Sci. U. S. A. *102,* 7292-7296.

Bardor, M., Loutelier-Bourhis, C., Paccalet, T., Cosette, P., Fitchette, A.C., Vezina, L.P., Trepanier, S., Dargis, M., Lemieux, R., Lange, C., Faye, L., and Lerouge, P. (2003). Monoclonal C5-1 antibody produced in transgenic alfalfa plants exhibits a N-glycosylation that is homogenous and suitable for glyco-engineering into human-compatible structures. Plant Biotechnol. J. *1,* 451-462.

Barnes, D., and Sato, G. (1980). Methods for growth of cultured cells in serum-free medium. Anal. Biochem. *102,* 255-270.

Beutler, E., Gelbart, T., Lee, P., Trevino, R., Fernandez, M.A., and Fairbanks, V.F. (2000). Molecular characterization of a case of atransferrinemia. Blood *96,* 4071-4074.

Boehm, R. (2007). Bioproduction of therapeutic proteins in the 21st century and the role of plants and plant cells as production platforms. Ann. N. Y. Acad. Sci. *1102,* 121-134.

Brereton, H.M., Chamberlain, D., Yang, R., Tea, M., McNeil, S., Coster, D.J., and Williams, K.A. (2007). Single chain antibody fragments for ocular use produced at high levels in a commercial wheat variety. J. Biotechnol. *129,* 539-546.

Bullen, J.J. (1981). The significance of iron in infection. Rev. Infect. Dis. *3,* 1127-1138.

Bullen, J.J., Rogers, H.J., and Griffiths, E. (1978). Role of iron in bacterial infection. Curr. Top. Microbiol. Immunol. *80,* 1-35.

Bulotta, A., Farilla, L., Hui, H., and Perfetti, R. (2004). The role of GLP-1 in the regulation of islet cell mass. Cell Biochem. Biophys. *40,* 65-78.

Cho, M.J., Yano, H., Okamoto, D., Kim, H.K., Jung, H.R., Newcomb, K., Le, V.K., Yoo, H.S., Langham, R., Buchanan, B.B., and Lemaux, P.G. (2004). Stable transformation of rice (*Oryza sativa L.*) via microprojectile bombardment of highly regenerative, green tissues derived from mature seed. Plant Cell Rep. *22,* 483-489.

Cramer, C.L., Weissenborn, D.L., Oishi, K.K., Grabau, E.A., Bennett, S., Ponce, E., Grabowski, G.A., and Radin, D.N. (1996). Bioproduction of human enzymes in transgenic tobacco. Ann. N. Y. Acad. Sci. *792,* 62-71.

Daniell, H. (2006). Production of biopharmaceuticals and vaccines in plants via the chloroplast genome. Biotechnol. J. *1,* 1071-1079.

Daniell, H., Streatfield, S.J., and Wycoff, K. (2001). Medical molecular farming: production of antibodies, biopharmaceuticals and edible vaccines in plants. Trends Plant Sci. *6,* 219-226.

Daugherty, A.L., and Mrsny, R.J. (1999). Transcellular uptake mechanisms of the intestinal epithelial barrier Part one. Pharm. Sci. Technolo. Today *4,* 144-151.

de Vries, B., Walter, S.J., von Bonsdorff, L., Wolfs, T.G., van Heurn, L.W., Parkkinen, J., and Buurman, W.A. (2004). Reduction of circulating redox-active iron by apotransferrin protects against renal ischemia-reperfusion injury. Transplantation *77,* 669-675.

Drucker, D.J. (2003). Enhancing incretin action for the treatment of type 2 diabetes. Diabetes Care *26,* 2929-2940.

Edwards, C.M. (2005). The GLP-1 system as a therapeutic target. Ann. Med. *37,* 314-322.

Ellison, R.T.,3rd, Giehl, T.J., and LaForce, F.M. (1988). Damage of the outer membrane of enteric gram-negative bacteria by lactoferrin and transferrin. Infect. Immun. *56,* 2774-2781.

Funk, W.D., MacGillivray, R.T., Mason, A.B., Brown, S.A., and Woodworth, R.C. (1990). Expression of the amino-terminal half-molecule of human serum transferrin in cultured cells and characterization of the recombinant protein. Biochemistry *29,* 1654-1660.

Gellissen, G., Melber, K., Janowicz, Z.A., Dahlems, U.M., Weydemann, U., Piontek, M., Strasser, A.W., and Hollenberg, C.P. (1992). Heterologous protein production in yeast. Antonie Van Leeuwenhoek *62,* 79-93.

Hamman, J.H., Enslin, G.M., and Kotze, A.F. (2005). Oral delivery of peptide drugs: barriers and developments. BioDrugs *19,* 165-177.

Han, H.K., and Amidon, G.L. (2000). Targeted prodrug design to optimize drug delivery. AAPS Pharm. Sci. *2,* E6.

Hayashi, A., Wada, Y., Suzuki, T., and Shimizu, A. (1993). Studies on familial hypotransferrinemia: unique clinical course and molecular pathology. Am. J. Hum. Genet. *53,* 201-213.

Holst, J.J. (2007). The physiology of glucagon-like peptide 1. Physiol. Rev. *87,* 1409-1439.

Holst, J.J., and Gromada, J. (2004). Role of incretin hormones in the regulation of insulin secretion in diabetic and nondiabetic humans. Am. J. Physiol. Endocrinol. Metab. *287,* E199-206.

Hou, J., Yan, R., Ding, D., Yang, L., Wang, C., Wu, Z., Yu, X., Li, W., and Li, M. (2007a). Oral administration of a fusion protein containing eight GLP-1 analogues produced in *Escherichia coli* BL21(DE3) in streptozotocin-induced diabetic rats. Biotechnol. Lett. *29,* 1439-1446.

Hou, J., Yan, R., Yang, L., Wu, Z., Wang, C., Ding, D., Li, N., Ma, C., and Li, M. (2007b). High-level expression of fusion protein containing 10 tandem repeated GLP-1 analogs in yeast *Pichia pastoris* and its biological activity in a diabetic rat model. Biosci. Biotechnol. Biochem. *71,* 1462-1469.

Huebers, H.A., and Finch, C.A. (1987). The physiology of transferrin and transferrin receptors. Physiol. Rev. *67,* 520-582.

Hwa Kim, S., Hoon Jeong, J., Joe, C.O., and Gwan Park, T. (2005). Folate receptor mediated intracellular protein delivery using PLL-PEG-FOL conjugate. J. Control. Release *103,* 625-634.

Ikeda, R.A., Bowman, B.H., Yang, F., and Lokey, L.K. (1992). Production of human serum transferrin in *Escherichia coli.* Gene *117,* 265-269.

Kaminski, K.A., Bonda, T.A., Korecki, J., and Musial, W.J. (2002). Oxidative stress and neutrophil activation--the two keystones of ischemia/reperfusion injury. Int. J. Cardiol. *86,* 41-59.

Kimmerlin, T., and Seebach, D. (2005). '100 Years of peptide synthesis': ligation methods for peptide and protein synthesis with applications to beta-peptide assemblies. J. Pept. Res. *65,* 229-260.

Lesnikov, V., Lesnikova, M., and Deeg, H.J. (2001). Pro-apoptotic and anti-apoptotic effects of transferrin and transferrin-derived glycans on hematopoietic cells and lymphocytes. Exp. Hematol. *29,* 477-489.

Li, H., and Qian, Z.M. (2002). Transferrin/transferrin receptor-mediated drug delivery. Med. Res. Rev. *22,* 225-250.

Lim, C.J., and Shen, W.C. (2005). Comparison of monomeric and oligomeric transferrin as potential carrier in oral delivery of protein drugs. J. Control. Release *106,* 273-286.

Ma, S.W., Zhao, D.L., Yin, Z.Q., Mukherjee, R., Singh, B., Qin, H.Y., Stiller, C.R., and Jevnikar, A.M. (1997). Transgenic plants expressing autoantigens fed to mice to induce oral immune tolerance. Nat. Med. *3,* 793-796.

MacGillivray, R.T., Moore, S.A., Chen, J., Anderson, B.F., Baker, H., Luo, Y., Bewley, M., Smith, C.A., Murphy, M.E., Wang, Y., Mason, A.B., Woodworth, R.C., Brayer, G.D., and Baker, E.N. (1998). Two high-resolution crystal structures of the recombinant N-lobe of human transferrin reveal a structural change implicated in iron release. Biochemistry *37,* 7919-7928.

Mason, A.B., He, Q.Y., Adams, T.E., Gumerov, D.R., Kaltashov, I.A., Nguyen, V., and MacGillivray, R.T. (2001). Expression, purification, and characterization of recombinant nonglycosylated human serum transferrin containing a C-terminal hexahistidine tag. Protein Expr. Purif. *23,* 142-150.

Mason, A.B., Miller, M.K., Funk, W.D., Banfield, D.K., Savage, K.J., Oliver, R.W., Green, B.N., MacGillivray, R.T., and Woodworth, R.C. (1993). Expression of glycosylated and nonglycosylated human transferrin in mammalian cells. Characterization of the recombinant proteins with comparison to three commercially available transferrins. Biochemistry *32,* 5472-5479.

Menassa, R., Du, C., Yin, Z.Q., Ma, S., Poussier, P., Brandle, J., and Jevnikar, A.M. (2007). Therapeutic effectiveness of orally administered transgenic low-alkaloid tobacco expressing human interleukin-10 in a mouse model of colitis. Plant. Biotechnol. J. *5,* 50-59.

Nauck, M.A., Heimesaat, M.M., Orskov, C., Holst, J.J., Ebert, R., and Creutzfeldt, W. (1993). Preserved incretin activity of glucagon-like peptide 1 [7-36 amide] but not of synthetic human gastric inhibitory polypeptide in patients with type-2 diabetes mellitus. J. Clin. Invest. *91,* 301-307.

Pavlou, A.K., and Reichert, J.M. (2004). Recombinant protein therapeutics--success rates, market trends and values to 2010. Nat. Biotechnol. *22,* 1513-1519.

Russell-Jones, G.J. (2004). Use of targeting agents to increase uptake and localization of drugs to the intestinal epithelium. J. Drug Target. *12,* 113-123.

Saffran, M., Pansky, B., Budd, G.C., and Williams, F.E. (1997). Insulin and the gastrointestinal tract. J. Control. Release *46,* 89-98.

Salamat-Miller, N., and Johnston, T.P. (2005). Current strategies used to enhance the paracellular transport of therapeutic polypeptides across the intestinal epithelium. Int. J. Pharm. *294,* 201-216.

Sandhu, J.S., Krasnyanski, S.F., Domier, L.L., Korban, S.S., Osadjan, M.D., and Buetow, D.E. (2000). Oral immunization of mice with transgenic tomato fruit expressing respiratory syncytial virus-F protein induces a systemic immune response. Transgenic Res. *9,* 127-135.

Schillberg, S., Twyman, R.M., and Fischer, R. (2005). Opportunities for recombinant antigen and antibody expression in transgenic plants--technology assessment. Vaccine *23,* 1764-1769.

Shah, D., and Shen, W.C. (1996). Transcellular delivery of an insulin-transferrin conjugate in enterocyte-like Caco-2 cells. J. Pharm. Sci. *85,* 1306-1311.

Singh, R., Singh, S., and Lillard, J.W. Jr. (2008). Past, present, and future technologies for oral delivery of therapeutic proteins. J. Pharm. Sci. *97,* 2497-2523.

Smith, H.E. (2007). The transcriptional response of *Escherichia coli* to recombinant protein insolubility. J. Struct. Funct. Genomics *8,* 27-35.

Steinlein, L.M., Graf, T.N., and Ikeda, R.A. (1995). Production and purification of N-terminal half-transferrin in *Pichia pastoris*. Protein Expr. Purif. *6,* 619-624.

Sugita, K., Endo-Kasahara, S., Tada, Y., Lijun, Y., Yasuda, H., Hayashi, Y., Jomori, T., Ebinuma, H., and Takaiwa, F. (2005). Genetically modified rice seeds accumulating GLP-1 analogue stimulate insulin secretion from a mouse pancreatic beta-cell line. FEBS Lett. *579,* 1085-1088.

Trehin, R., and Merkle, H.P. (2004). Chances and pitfalls of cell penetrating peptides for cellular drug delivery. Eur. J. Pharm. Biopharm. *58,* 209-223.

Varma, M.V., Ashokraj, Y., Dey, C.S., and Panchagnula, R. (2003). P-glycoprotein inhibitors and their screening: a perspective from bioavailability enhancement. Pharmacol. Res. *48,* 347-359.

Wang, D.J., Brandsma, M., Yin, Z., Wang, A., Jevnikar, A.M., and Ma, S. (2008). A novel platform for biologically active recombinant human interleukin-13 production. Plant. Biotechnol. J. *6,* 504-515.

Ward, P.D., Tippin, T.K., and Thakker, D.R. (2000). Enhancing paracellular permeability by modulating epithelial tight junctions. Pharm. Sci. Technolo. Today *3,* 346-358.

Widera, A., Bai, Y., and Shen, W.C. (2004). The transepithelial transport of a G-CSF-transferrin conjugate in Caco-2 cells and its myelopoietic effect in BDF1 mice. Pharm. Res. *21,* 278-284.

Widera, A., Kim, K.J., Crandall, E.D., and Shen, W.C. (2003). Transcytosis of GCSF-transferrin across rat alveolar epithelial cell monolayers. Pharm. Res. *20,* 1231-1238.

Xia, C.Q., Wang, J., and Shen, W.C. (2000). Hypoglycemic effect of insulin-transferrin conjugate in streptozotocin-induced diabetic rats. J. Pharmacol. Exp. Ther. *295,* 594-600.

Yasuda, H., Hayashi, Y., Jomori, T., and Takaiwa, F. (2006). The correlation between expression and localization of a foreign gene product in rice endosperm. Plant Cell Physiol. *47,* 756-763.

Yasuda, H., Tada, Y., Hayashi, Y., Jomori, T., and Takaiwa, F. (2005). Expression of the small peptide GLP-1 in transgenic plants. Transgenic Res. *14,* 677-684.

Zeitlin, L., Olmsted, S.S., Moench, T.R., Co, M.S., Martinell, B.J., Paradkar, V.M., Russell, D.R., Queen, C., Cone, R.A., and Whaley, K.J. (1998). A humanized monoclonal antibody produced in transgenic plants for immunoprotection of the vagina against genital herpes. Nat. Biotechnol. *16,* 1361-1364.

Zhong, Q., Xu, L., Zhang, C., and Glatz, C.E. (2007). Purification of recombinant aprotinin from transgenic corn germ fraction using ion exchange and hydrophobic interaction chromatography. Appl. Microbiol. Biotechnol. *76,* 607-613.

Zorko, M., and Langel, U. (2005). Cell-penetrating peptides: mechanism and kinetics of cargo delivery. Adv. Drug Deliv. Rev. *57,* 529-545.

Chapter 2

A proficient approach to the production of therapeutic glucagon-like peptide-1 (GLP-1) in transgenic plants

---

2.1 Introduction

The gastrointestinal GLP-1 hormone has recently attracted much attention for its pleiotropic therapeutic effects and potential to treat symptoms associated with Type II diabetes (Holst, 2007). In rats and mice, therapeutic GLP-1 administration increases beta-cell mass, making it possible to reverse beta-cell damage occurring as a result of Type II diabetes (Bulotta *et al.*, 2004). In addition, GLP-1 treatment decreases glucose levels, stimulates insulin secretion and insulin sensitivity, decreases glucagon secretion, promotes weight loss, delays gastric emptying and limits food intake (appetite suppression) in both humans and animals (Drucker, 2003; Edwards, 2005; Nauck *et al.*, 1993). The insulinotropic activity of GLP-1 is glucose-dependent, thereby lessening, but likely not alleviating, the risk of hypoglycaemia which is often associated with sulfonylurea treatment, one of the most commonly used therapies for treatment of Type II diabetes (Edwards *et al.*, 1998; Nathan *et al.*, 1992). The GLP-1 peptide is naturally synthesized from intestinal endocrine L cells by prohormone convertase 1 (PC1)-mediated posttranslational processing of proglucagon, and exists in two biologically relevant forms: the principal amidated active form of GLP-1 (amino acids

7-36) and unamidated GLP-1 (amino acids 7-37) (Holst, 2007). Chemical synthesis is the most commonly used method for production of therapeutic peptides including GLP-1 (Latham, 1999). However, this method is expensive and often produces low yields of active peptide product. The use of recombinant DNA technology offers the possibility of producing these peptides inexpensively and in large quantities.

Currently, both yeast and bacterial bioreactors have been demonstrated to produce rGLP-1 (Hou *et al.*, 2007a, b). While both microbial systems exhibit some advantages over traditional chemical synthesis methods for GLP-1 production, conventional cell culture-based expression systems have serious limitations. One such limitation is the ability to scale up rGLP-1 production, as microbial and cell-based production platforms necessitate sophisticated fermentation equipment and facilities, requiring a substantial amount of capital investment. In addition, rGLP-1 accumulated in microbial-based bioreactors often requires extensive purification prior to therapeutic use, so as to remove endogenous host proteins and other compounds such as bacterial endotoxins. Taken together, the infrastructure needed for fermentation and the protein purification necessary for recombinant product recovery, contribute to the high cost of rGLP-1 production in microbial-based systems. As a result, the plant bioreactor may prove to be a suitable alternative to microbial and cell-based methods for rGLP-1 generation due to its many inherent production benefits as outlined in section 1.2.3.

The expression of rGLP-1 has been reported in transgenic rice (Sugita *et al.*, 2005; Yasuda *et al.*, 2005, 2006). Originally, no recombinant protein was detected in rice seeds when rGLP-1 was expressed as a monomer fused to the signal peptide of glutelin (a rice storage protein), possibly due to siRNA mediated gene silencing and/or peptide

instability and proteolytic degradation (Yasuda *et al.*, 2005). Subsequently, the accumulation of rGLP-1 was demonstrated in rice seeds when it was expressed as a fusion protein with globulin (another rice seed storage protein) (Sugita *et al.*, 2005). As the biological activity of the globulin-GLP-1 fusion protein was demonstrated only after the physical release of GLP-1 from the fusion protein by *in vitro* enzymatic digestion, it was speculated that the recombinant fusion protein might have reduced GLP-1 biological activity. Recently, rGLP-1 was demonstrated to accumulate in rice seeds when expressed as a pentamer repeat fused to the signal peptide of rice glutelin or chitinase (Yasuda *et al.*, 2006). However, based on immunoblot analysis, the rice seed-derived recombinant protein is smaller in size than that calculated for a synthetic rGLP-1 pentamer, most likely attributed to incorrect processing of the incorporated plant signal peptide (Yasuda *et al.*, 2006). Furthermore, no data were provided demonstrating the biological activity of the recombinant seed-based GLP-1 pentamer (Yasuda *et al.*, 2006).

In the present study, a new approach for the production of biologically active rGLP-1 in transgenic tobacco plants is reported. This novel production scheme is based on the expression of rGLP-1 as a protein multimer consisting of ten sequential tandem copies of *GLP-1*. Here, it is shown rGLP-1 decamer protein was stably expressed and accumulated to relatively high levels in transgenic tobacco plants. More importantly, plant-derived rGLP-1, retained as a synthetic decamer, remains biologically active as demonstrated by its ability to stimulate insulin secretion from a mouse pancreatic beta-cell line (MIN6) *in vitro*.

2.2 Materials and Methods

2.2.1 Synthetic gene and expression plasmid construction

Construction of the synthetic gene encoding ten sequential repeats of *GLP-1* involved the PCR amplification of *GLP-1* using three separate primer sets to generate fragments with partially overlapping, complementary ends.* As shown in Figure 2.1A, three separate *GLP-1* DNA fragments designated as Start, Link and Stop were initially generated using three different primer pairs, each amplifying a single 90 bp *GLP-1* open reading frame. The Start fragment was created using the forward primer P1 (5'AATT**CCATGG**GGCATTCTGAGGGAACCTTCACCTCTGACG-3') and reverse primer P2 (5'-AATTGAATTCAATTCTCGAGCCTTCCCTTCACCACCAAGC-3'). Forward primer P1 contained a 5' *Nco*I restriction site (bold) used as the start codon, while reverse primer P2 contained a 3' *Xho*I (double underline) restriction site for subsequent gene fusion. The Link fragment was obtained using forward primer P3 (5'-AATT**GTCGAC**CATTCTGAGGGAACCTTCACCTCTGACG-3') containing a 5' *Sal*I restriction site (bold) and reverse primer P2. Finally, the Stop fragment was generated using forward primer P3 and reverse primer P4 (5'-AATTCTCGAG**TTA**ATG ATGATGATGATGATGCCTTCCCTTCACCAACCAAGC-3'). Primer P4 contained a 3' 6xHis tag (double underline), stop codon (bold) and *Xho*I restriction site (underline) for subsequent gene-fragment fusions. All PCR amplifications were performed using a PCR Sprint Thermal Cycler (Thermo Fischer Scientific Inc., Waltham, MD, USA)

---

* For further information on bacterial strains, plasmid extraction, ligation and bacterial transformation procedures, refer to Appendix 1.

performed under identical conditions: denature at 94°C for 1 min, anneal at 55°C for 45 s and elongate at 72°C for 35 s, for a total of 35 cycles followed by a final elongation at 72°C for 10 min.

The generation of the *GLP-1* decamer repeat was completed using single step-by-step ligation of the Start, Link and Stop *GLP-1* monomer fragments. Initially, one Link fragment was fused to the Start fragment using *SalI/Xho*I restriction sites to generate a *GLP-1* dimer repeat. When ligated, the compatible ends of the *SalI/Xho*I pair produce a sequence that is recognized by neither restriction enzyme. A second Link fragment was then ligated to the 3' end of the *GLP-1* dimer repeat using identical *SalI/Xho*I restriction sites to generate a *GLP-1* trimer repeat, again destroying both restriction sites in the process. This step was repeated six more times until a sequence composed of nine *GLP-1* repeats (1 Start fragment + 8 Link fragments) was generated. The final step consisted of ligating the Stop fragment to the 3' end of the final Link fragment via *SalI/Xho*I restriction sites to generate the final *GLP-1* decamer sequence, designated as *GLP-1x10* (see Figure 2.1B). The sequence integrity of synthetic *GLP-1x10* was confirmed by DNA sequencing (Sequencing Facility, Robarts Research Institute, London, ON).

The *GLP-1x10* plant expression vector was generated by incorporating *GLP-1x10* into plasmid pRTL (Carrington and Freed, 1990) via *Nco*I and *Xho*I restriction sites. Plasmid pRTL contains an enhanced constitutive cauliflower mosaic virus (CaMV) 35S promoter in tandem as well as a tobacco etch virus (TEV) 5'UTL and the 3'UTR sequence of the nopaline synthase (NOS) gene. The entire *GLP-1x10* expression cassette was ligated into the plant binary expression vector pBIN19 (Bevan, 1984) to generate the final expression plasmid pALP-GLP-1x10 (Figure 2.1C). Plasmid pBIN19 contains both

left and right border regions necessary for *Agrobacterium*-mediated gene transfer as well as the neomycin phosphotransferase II (*NPT-II*) gene under control of the *NOS* promoter conferring kanamycin resistance.

2.2.2 Generation of transgenic plants

Plant binary expression vector pALP-GLP-1x10 was introduced into *Agrobacterium tumefaciens* strain LBA4404 using tri-parental mating (Wise *et al.*, 2006) with *E. coli* containing helper plasmid pRK2013 (Bio-Rad Laboratories, Hercules, CA, USA). Low-alkaloid *Nicotiana tabacum* cv. 81V9 was transformed with *A. tumefaciens* harboring pALP-GLP-1x10 according to the method of Horsch *et al.*, (1985). Primary transgenic plants were selected on MS medium containing kanamycin (100 mg/L). As regenerated plants matured, they were transferred into a greenhouse and maintained for further analysis. For information regarding specific procedures used for tri-parental mating and tobacco leaf-disc transformation, refer to Appendix 1.6 and 1.7 respectively.

2.2.3 Screening of putative transgenic plants by PCR and RT-PCR

Total genomic DNA (gDNA) was extracted from individual regenerated tobacco plants using a basic phenol/chloroform extraction. For an outline of the gDNA extraction procedure, please refer to Appendix 1.8. Total tobacco gDNA was subjected to PCR to confirm stable integration of *GLP-1x10* into the tobacco nuclear genome. The first initial PCR reaction utilized forward primer P3 and reverse primer P4 to allow for elongation of all possible repeat lengths of the *GLP-1* decamer. A second PCR reaction using reverse primer P4 along with a forward primer corresponding to the TEV 5' UTL (5'-CGAATCT

CAAGCAATCAAGC-3') designated as P5, was used to obtain a single fragment length of the *GLP-1* decamer (1072 bp). Both PCR reactions were subjected to 35 cycles of denature at 95°C for 55 s, anneal at 67°C for 47 s and elongate at 72°C for 1 min, with a final elongation at 72°C for 10 min. All PCR samples were separated by electrophoresis on a 0.75% (w/v) agarose gel and analyzed by UV visualization using ethidium bromide staining.

For reverse transcriptase (RT)-PCR analysis, total tobacco plant RNA was extracted using a Trizol reagent extraction kit (Invitrogen, Carlsbad, CA, USA) according to the manufacturer's instructions. To initiate first strand synthesis reactions, approximately 0.5 μg of oligo$(dT)_{12\text{-}18}$ primer was annealed to 5 μg of purified RNA in a total reaction volume of 12 μl for 10 min at 70°C. Generation of complementary (c)DNA was performed with addition of 20 U of SuperScript™ II RNase H Reverse Transcriptase (Invitrogen) subjected to a 50 min incubation at 42°C followed by an additional 15 min incubation at 70°C. Approximately 150 ng of first-strand synthesized cDNA was used as a template for PCR amplification in a 100 μl reaction volume using identical conditions and primers (P4 and P5) outlined for the detection of genome-integrated *GLP-1x10* in transgenic tobacco. All RT-PCR samples were separated by electrophoresis on a 0.75% (w/v) agarose gel and analyzed by UV visualization using ethidium bromide staining. PCR amplification was performed using identical primer pairs and reaction conditions (mentioned for RT-PCR reactions) on total RNA samples without first-strand cDNA synthesis as a negative control.

2.2.4 Immunoblot analysis

Tobacco plant-derived recombinant (r)GLP-1x10 accumulation was assessed by SDS-PAGE followed by immunoblotting. In brief, the uppermost fully expanded leaves of 6-week-old greenhouse-grown tobacco plants were homogenized in liquid nitrogen and resuspended in cold extraction buffer [25 mM tris(hydroxymethyl)aminomethane (Tris) pH 7.0, 50 mM NaCl, 2 mM β-mercaptoethanol, 1 mM phenyl-methylsulphonyl fluoride (PMSF), 2 μg/mL aprotinin, 2 μg/mL pepstatin A and 2 μg/mL leupeptin]. Samples were centrifuged at 12,000-x G for 10 min at 4°C, and the supernatant collected. The concentration of extracted total soluble protein (TSP) was determined by the method of Bradford using Bio-Rad protein assay dye reagent and bovine serum albumin (BSA) (Sigma-Aldrich, St. Louis, MO, USA) as a protein standard. Extracted tobacco TSP samples were boiled for 10 min in sample buffer [63 mM Tris-HCl, 2% (w/v) SDS, 10% (v/v) glycerol, 0.1 M dithiothreitol (DTT), 0.01% (w/v) bromophenol blue, pH 6.8] Proteins were separated on 12.5% (w/v) SDS-PAGE gels and transferred to polyvinylidene difluoride (PVDF) membranes (Millipore, Burlington, MA, USA) using a semi-dry transfer method. Commercially available GLP-1 standard (Sigma-Aldrich) was used as a positive control and was boiled first for 10 min in sample buffer (described above) and separated on a 17.5% (w/v) SDS-PAGE gel before transfer to PVDF and subsequent immunoblotting. Blots were blocked for 1 h in 5% (w/v) skim milk-TBST [20 mM Tris, 150 mM NaCl, 0.02% (v/v) Tween-20, pH 7.6] and incubated at room temperature for 2 h in a 1:500 dilution (v/v) of mouse anti-GLP-1 primary monoclonal antibody (Santa Cruz Biotechnology, Santa Cruz, CA, USA). Following washing in TBST, blots were incubated at room temperature for 1 h in goat anti-mouse IgG

secondary antibody conjugated with horseradish peroxidase (Sigma-Aldrich). The enhanced chemiluminescence (ECL) reaction kit (Amersham Pharmacia Biotech Inc., Piscataway, NJ, USA) was used according to the manufacturer's instructions for protein band detection.

2.2.5 ELISA quantification of plant-derived rGLP-1x10

The relative amount of tobacco-accumulated rGLP-1x10 protein was quantified using an indirect Enzyme Linked ImmunoSorbent Assay (ELISA) compared to known amounts of 6xHis-tagged reference protein. Briefly, total protein samples resuspended in sodium bicarbonate (pH 9.6) were coated on a 96-well mictrotiter plate and incubated overnight at 4°C. Wells were washed three times with PBST [phosphate buffered saline containing 0.05% (v/v) Tween-20] and blocked with 3% (w/v) BSA in PBST for 2 h at room temperature. After washing with PBST, rabbit anti-6xHis monoclonal antibody (Rockland Immunochemicals, Gilbertsville, PA, USA) diluted to 1:5000 was added and plates were incubated overnight at 4°C. After three consecutive PBST washes, horseradish peroxidase-conjugated goat anti-rabbit IgG (1:2000 (v/v)) secondary antibody (Sigma-Aldrich) was added and incubated at room temperature for 1 h. Enzyme substrate TMB (R&D Systems, Minneapolis, MN, USA) was added to each well (as per the manufacturer's instructions) and incubated at room temperature in the dark for 30 min. The substrate reaction was stopped with addition of 100 µL/well stop solution (R&D Systems). The optical density (OD) was measured at 450 nm in a microplate reader (Bio-Rad 3550), and converted as a percentage of plant TSP by reference to an ELISA standard curve constructed with the 6xHis-tagged reference protein.

2.2.6 Purification of His-tagged rGLP-1x10

Plant-derived rGLP-1x10 was purified from transgenic tobacco plant leaf extracts by histidine affinity chromatography using HiTrap Chelating HP columns (GE Healthcare, Chalfont St. Giles, UK) according to the manufacturer's instructions. Approximately 5 mL of tobacco TSP, extracted as described in section 2.2.5, was collected and loaded into the HiTrap Chelating HP column and subsequently washed with wash buffer [10 mM imidazole, 20 mM Na_2HPO_4, 500 mM NaCl]. The bound plant-derived rGLP-1x10 was eluded using elution buffer [500 mM imidazole, 20 mM Na_2HPO_4, 500 mM NaCl] with subsequent 1 mL fractions collected for analysis. Eluted rGLP-1x10 fractions were dialyzed extensively against PBS [4.3 mM Na_2HPO_4, 137 mM NaCl, 2.7 mM KCl, 1.4 mM KH_2PO_4, pH 7.4] and concentrated using a speed vacuum at 4°C.

2.2.7 Biological activity assay of plant-derived rGLP-1x10

The biological activity of plant-derived rGLP-1x10 was determined by its ability to stimulate insulin secretion from a mouse pancreatic beta-cell line, MIN6 (Miyazaki *et al.*, 1990). In brief, MIN6 cells, a kind gift from Dr. Junichi Miyazaki (Osaka University, Osaka, JPN) were cultured and maintained in 25 cm^2 tissue culture flasks using high-glucose Dulbecco's Modified Eagle Media (DMEM) supplemented with 15% (v/v) fetal calf serum, 100 U/mL penicillin, 0.1 mg/mL streptomycin, and 2 mM L-glutamine at 37°C in an atmosphere of humidified air (95%) and CO_2 (5%). The culture medium was replaced with fresh medium every 24 h and cells were used for experiments once they had reached 80% confluence. To determine the insulin-stimulating

effect of plant-derived rGLP-1x10 on MIN6 cells, the cells were washed with PBS and harvested using Trypsin-EDTA solution [0.125 M trypsin, 0.05 mg/ml EDTA] for 3 to 5 min. Harvesting was stopped with the addition of DMEM and subsequent centrifugation (1,500 rpm for 5 min). Cell pellets were resuspended in 10% (v/v) DMEM containing 10 mM glucose and counted using a hemacytometer. Cells were then added to each 1.5 ml culture tube (~1 x 10^6 cells/tube) containing 1.2 ml 10% (v/v) DMEM medium in the presence of 10 mM glucose plus His-purified plant-derived rGLP-1x10 (250 ng/mL), commercial GLP-1 (250 ng/mL) standard (Sigma-Aldrich), His-purified wild-type 81V9 TSP (250 ng/mL), or DMEM only. MIN6 cells were incubated for 135 min at 37°C, with culture supernatants subsequently collected and assayed for insulin concentration using an insulin ELISA kit (Crystal Chem Inc., Downers Grove, IL, USA) according to the manufacturer's instructions.

2.3 Results

2.3.1 Production of synthetic *GLP-1x10*, expression vector and transgenic plants

Design and construction of the synthetic *GLP-1x10* gene and expression vector pALP-GLP-1x10 is described in section 2.2.1. As shown in Figure 2.1C, the expression of *GLP-1x10* is under the control of the strong constitutive CaMV 35S promoter in tandem followed by a TEV 5' UTL, aiding in transgenic gene translation enhancement (Carrington and Freed, 1990). The addition of a 6xHis tag to the C-terminus of rGLP-1x10 was intended to facilitate purification of recombinant GLP-1 via immobilized metal affinity chromatography (IMAC).

Figure 2.1

Construction of GLP-1x10 decamer and plant expression vector pALP-GLP-1x10. (A) Three initial *GLP-1* DNA fragments (Start, Link, and Stop) were used to build the *GLP-1* sequence decamer, each containing a single *GLP-1* coding sequence and various 5' and 3' additions: P1 – forward primer containing *Nco*I, P2 – reverse primer containing *Xho*I, P3 – forward primer containing *Sal*I, P4 – reverse primer containing 6xHis tag and stop codon (TAA). (B) Final *GLP-1* decamer sequence generated from Start, Link, and Stop fragments. Each Link or Stop fragment was added consecutively to the Start fragment using *Sal*I/*Xho*I restriction sites to generate the final product. (C) Plant binary transformation vector pALP-GLP-1x10: LB – left border, P_{NOS} – nopaline synthase promoter, NPT-II – neomycin phosphotransferase II marker, T_{NOS} – nopaline synthase terminator, CaMV 35S x 2 – double constitutive cauliflower mosaic virus 35S promoter, TEV – tobacco etch virus UTL sequence, GLP-1x10 – 10 consecutive repeats of *GLP-1*, 6xHis – C-terminal His-purification tag, RB – right border. Note: diagram is not drawn to scale.

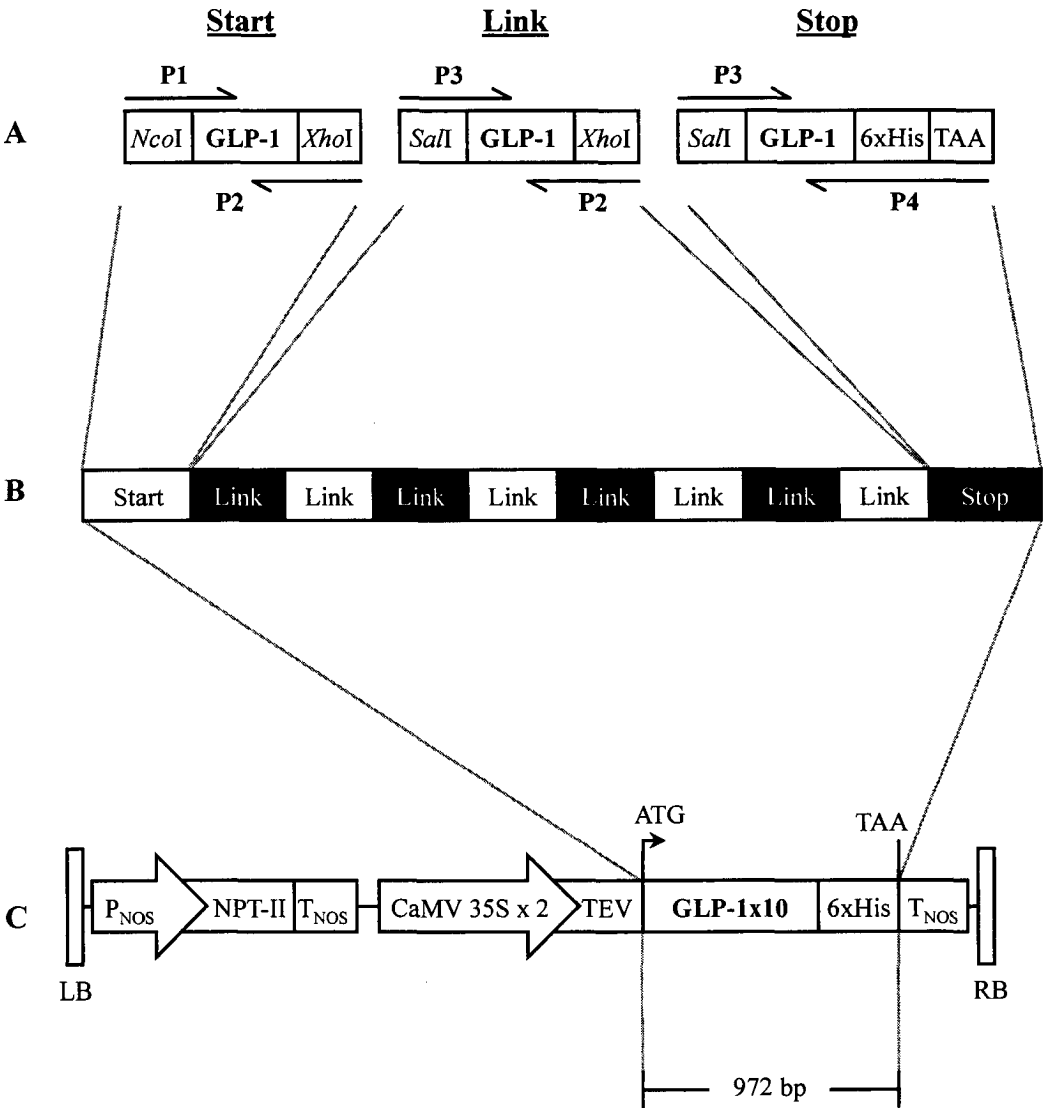
Start
Link
Stop
A
P1
P3
P3
NcoI
GLP-1
XhoI
SalI
GLP-1
XhoI
SalI
GLP-1
6xHis
TAA
P2
P2
P4
B
Start
Link
Link
Link
Link
Link
Link
Link
Link
Stop
ATG
TAA
C
P NOS
NPT-II
T NOS
CaMV 35S x 2
TEV
GLP-1x10
6xHis
T NOS
LB
RB
972 bp

The low alkaloid *N. tabacum* cultivar 81V9 was transformed with *A. tumefaciens* containing plasmid pALP-GLP-1x10 using a standard leaf-disc co-cultivation procedure (Horsch *et al.*, 1985). More than 25 independent transgenic tobacco plant lines were generated. There were no observed phenotypic differences between transgenic and untransformed 81V9 control plants. To confirm the integration of *GLP-1x10* into the tobacco nuclear genome, two separate PCR reactions were performed using total gDNA extracted from individual transgenic tobacco plant lines transformed with pALP-GLP-1x10. The first PCR demonstrates the existence of the *GLP-1* repeat, as all forms of *GLP-1x10* (from monomer to decamer), are amplified with use of primers P3 and P4 (Figure 2.2A). The second PCR reaction ensures that inserted *GLP-1x10* was intact. Amplification of total transgenic tobacco gDNA extracted from individual transgenic tobacco plant lines transformed with pALP-GLP-1x10 using primers P4 and primer P5 did indeed yield a single PCR product of expected size (1072 bp) for *GLP-1x10* (Figure 2.2B).

2.3.2 *GLP-1x10* transcripts accumulate in transgenic plants

PCR-positive tobacco plants transformed with pALP-GLP-1x10, were analyzed at the transcript level RT-PCR using total extracted tobacco plant RNA as a template. Using primers P4 and P5, RT-PCR revealed the presence of a DNA fragment of expected size (1072 bp) (Figure 2.2C), suggesting that *GLP-1x10* transcripts accumulate in tobacco plants transformed with pALP-GLP-1x10. PCR amplification of all samples of extracted tobacco plant RNA without first-strand cDNA synthesis produced no fragments, eliminating the possibility of DNA contamination of the RNA samples (data not shown).

Figure 2.2

PCR and RT-PCR analysis of GLP-1x10 transgenic tobacco plants. Total gDNA was extracted from putative transgenic tobacco plants transformed with pALP-GLP-1x10. Resulting gDNA was used for PCR amplification using Taq polymerase and primers (A) P3 and P4 to generate all ten possible fragment sizes of *GLP-1x10* or (B) P4 and P5 to yield a single product representing that of the intact *GLP-1x10* decamer: pUC19-GLP-1x10 – positive pDNA control, 81V9 – untransformed wild-type tobacco control, T1-T19 – independent transgenic tobacco lines transformed with pALP-GLP-1x10. (C) Detection of *GLP-1x10* mRNA in transgenic tobacco plants transformed with pALP-GLP-1x10 by RT-PCR. Total RNA was extracted from putative transgenic tobacco plants and converted to cDNA. A total of 150 ng of cDNA was used for PCR amplification using Taq polymerase and primers P4 and P5 to generate a single product corresponding in size to *GLP-1x10*. The quality of cDNA was confirmed by PCR analysis using *actin* specific primers (see Table 2 for sequence). All arrows correspond to bands of interest. All numerical values to the left represent the size in base pairs (bp) of the DNA marker. All samples were separated by electrophoresis on 0.75% (w/v) agarose gels followed by UV visualization using ethidium bromide staining.

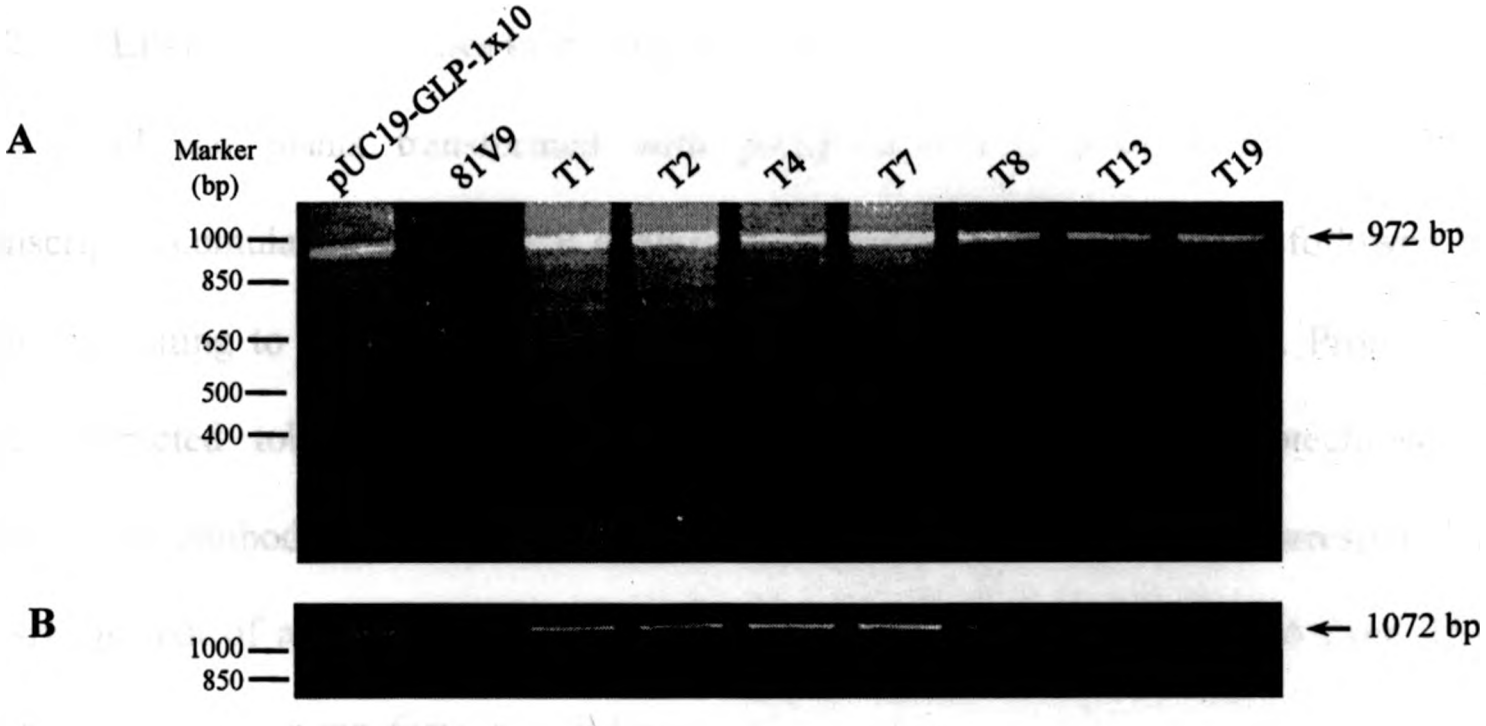
A
Marker
(bp)
pUC19-GLP-1x10
81V9
T1
T2
T4
T7
T8
T13
T19
1000
850
650
500
400
← 972 bp
B
1000
850
← 1072 bp

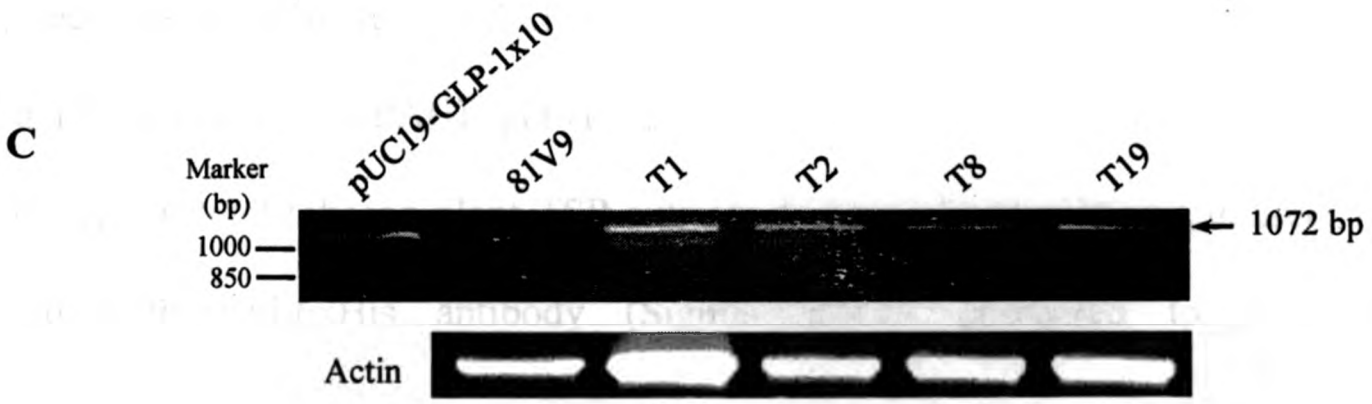
C
Marker
(bp)
pUC19-GLP-1x10
81V9
T1
T2
T8
T19
1000
850
← 1072 bp
Actin

The quality of tobacco plant generated cDNA was confirmed by PCR analysis using primers specific for *actin* (Figure 2.2C, Table 2).

2.3.3 rGLP-1x10 accumulates in transgenic plants

Tobacco plants transformed with pALP-GLP-1x10 positive for *GLP-1x10* transcript accumulation by RT-PCR analysis were subjected to SDS-PAGE followed by immunoblotting to verify the presence of accumulated rGLP-1x10 protein. Probing of total extracted tobacco plant TSP with anti-GLP-1 (Santa Cruz Biotechnology) monoclonal antibody identified a single ~36 kDa molecular weight band corresponding in size to that of a GLP-1 decamer (Figure 2.3B). No bands were detected from TSP extracted from untransformed wild-type 81V9 plants under identical conditions (Figure 2.3). Commercially available GLP-1 standard (Sigma-Aldrich) monomer peptide was used as a positive control to assess the affinity of the primary antibody. This GLP-1 monomer could be detected (~3.4 kDa) with use of long exposure during immunoblotting and a 17.5% (w/v) SDS-PAGE gel (Figure 2.3A). The relative accumulated amount of rGLP-1x10 in total tobacco plant TSP extracts was measured using an indirect ELISA method with anti-6xHis antibody (Sigma-Aldrich), compared to a quantified 6xHis-tagged reference protein. Relative accumulation levels of rGLP-1x10 were variable among individual transgenic tobacco plant lines, with lines T1, T7 and T19 being top producers and accumulating rGLP-1x10 at levels of nearly 0.15% of tobacco plant TSP (Figure 2.4).

Figure 2.3

Immunoblot analysis of tobacco-derived rGLP-1x10 protein. (A) Commercially available GLP-1 standard (Sigma-Aldrich) was separated (500 ng) by 17.5% (w/v) SDS-PAGE, transferred to PVDF membrane and probed with anti-GLP-1. Total soluble protein (TSP) was extracted from untransformed 81V9 tobacco and loaded (45 μg) as a control. The arrow labeled GLP-1 corresponds to the protein of interest: GLP-1 PC – GLP-1 positive control, 81V9 – untransformed wild-type tobacco control. (B) TSP extracted from tobacco transformed with pALP-GLP-1x10 and standardized to 45 μg, was separated by 12.5% (w/v) SDS-PAGE, transferred onto PVDF membrane and Immunoblotted with anti-GLP-1. The arrow labeled rGLP-1x10 corresponds to the recombinant protein of interest: T1-T7 – independent tobacco lines transformed with pALP-GLP-1x10. All numerical values to the left refer to the size in kilo Daltons of the protein marker. Following film development, blot (B) was stained with coomassie blue to verify equal loading.

A

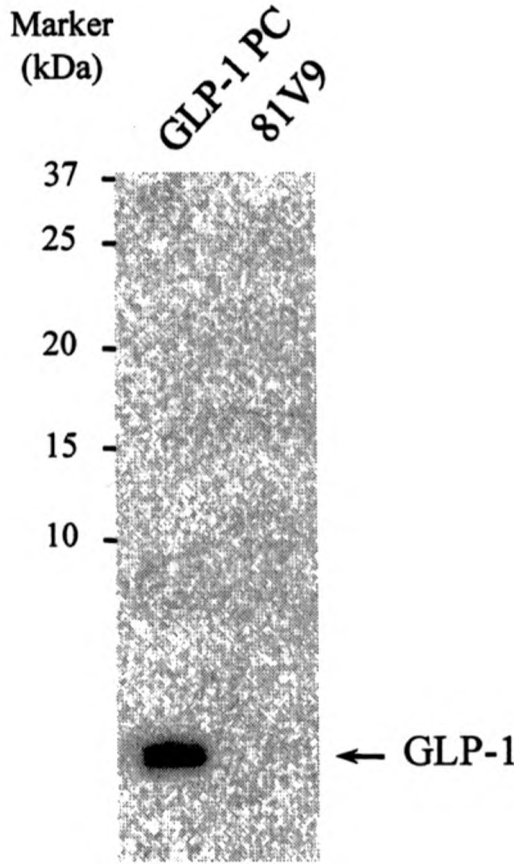
Marker
(kDa)
GLP-1 PC
81V9
37
25
20
15
10
GLP-1

B

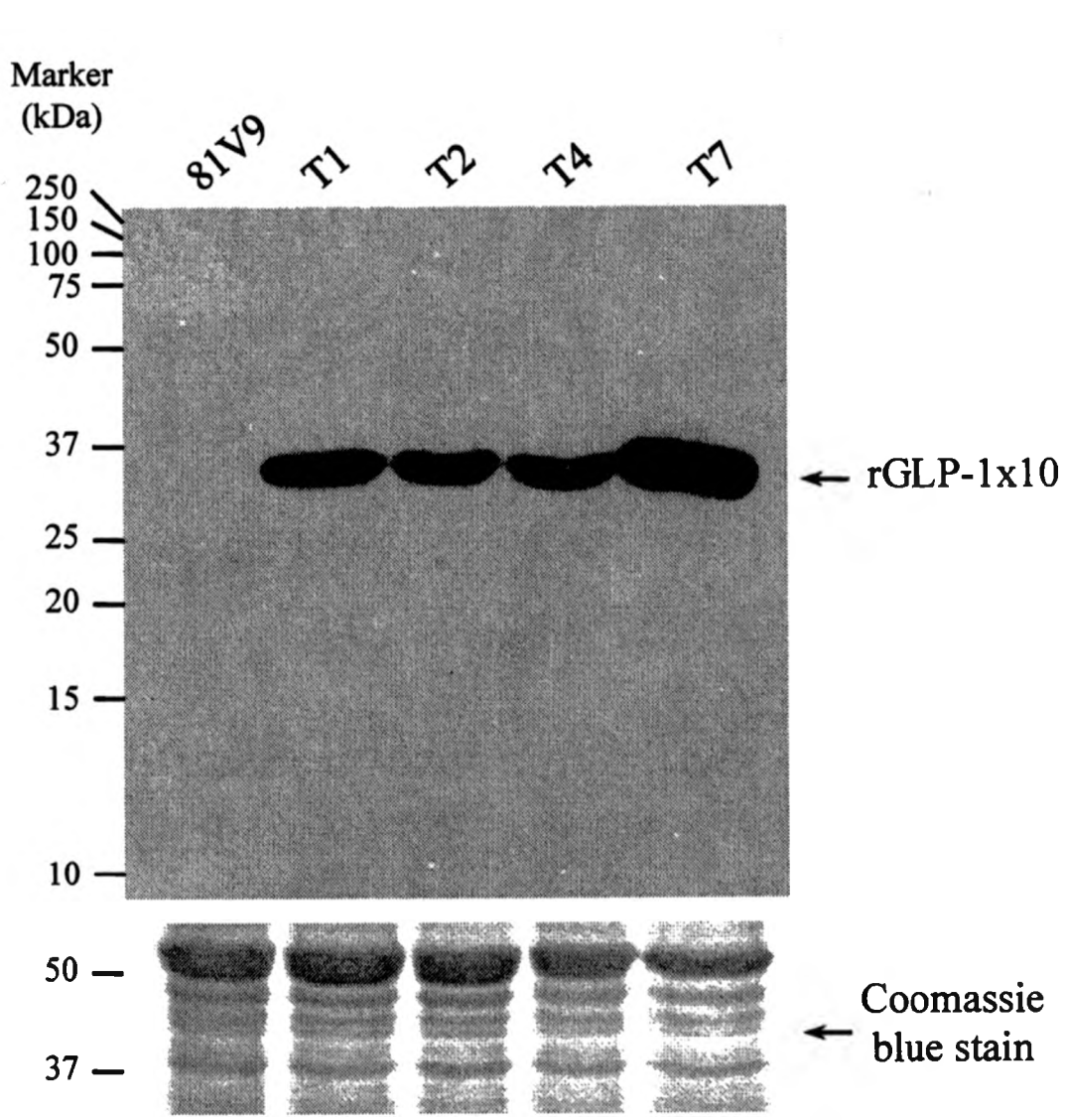
Marker
(kDa)
81V9
T1
T2
T4
T7
250
150
100
75
50
37
25
20
15
10
rGLP-1x10
50
37
Coomassie
blue stain

Figure 2.4

Quantification of rGLP-1x10 protein in transgenic tobacco by indirect ELISA. TSP extracted from leaves of tobacco transformed with pALP-GLP-1x10 was used to estimate the relative accumulation level of GLP-1x10 using indirect ELISA as described in section 2.2.5: T1-T23 – independent transgenic tobacco lines transformed with pALP-GLP-1x10. Data shown represents averages of three independent experiments. Error bars correspond to standard deviation.

ELISA quantification of tobacco-derived rGLP-1x10

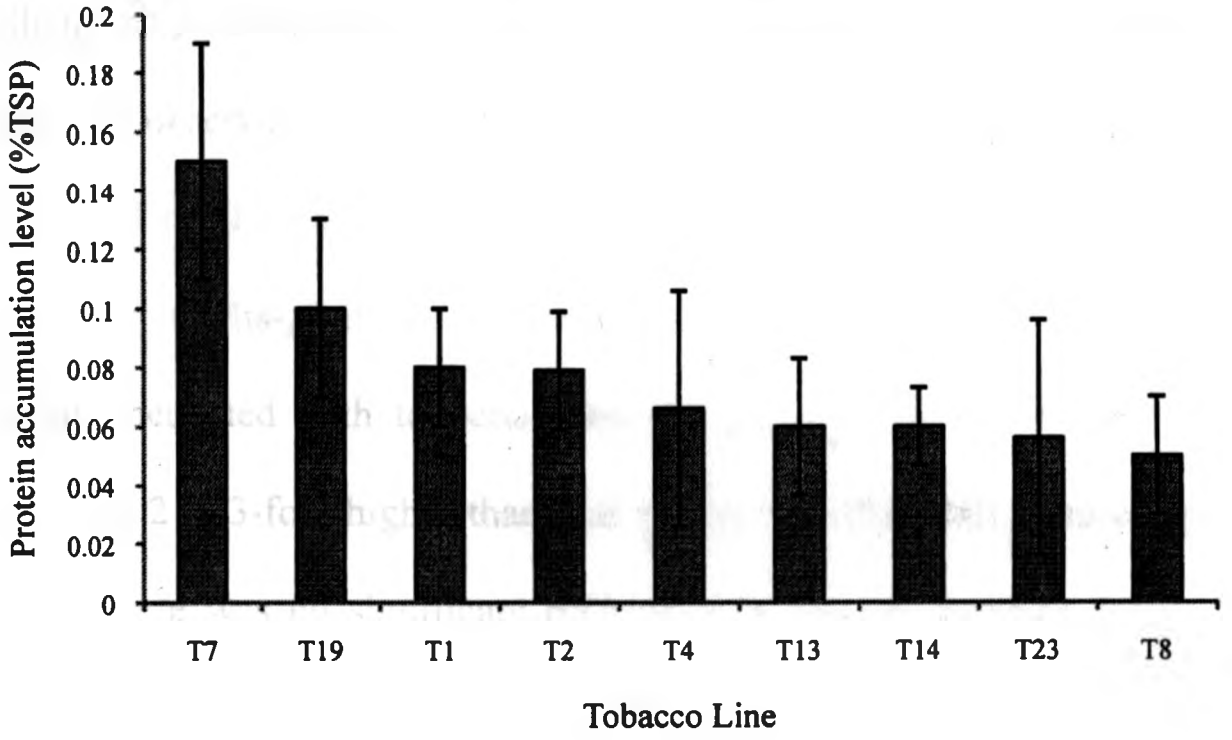

2.3.4 Plant-derived rGLP-1x10 is biologically active

As a primary therapeutic use of GLP-1 is to augment glucose-stimulated insulin secretion, plant-derived rGLP-1x10 was assessed for its ability to stimulate insulin release from a mouse pancreatic beta-cell line, MIN6. To this end, rGLP-1x10 was first purified by IMAC and checked by SDS-PAGE and immunoblotting to confirm its integrity (data not shown). Purified rGLP-1x10 protein was subsequently incubated in solution with MIN6 cells with insulin levels assessed by a direct insulin ELISA kit (Chrystal Chem Inc.). As shown in Figure 2.5A, a significant ($p<0.05$) increase in insulin concentration was observed in MIN6 cell-supernatant collected after 135 min incubation with plant-derived rGLP-1x10, as compared to MIN6 cell-supernatant incubated with medium only or 6xHis-purified wild-type 81V9 TSP. Insulin levels of MIN6 cell-supernatant incubated with tobacco plant-derived rGLP-1x10 reached as high as 69 ng/mL, a value 2 to 3-fold higher than that of control MIN6 cell culture supernatants (Figure 2.5A). There was no significant difference in insulin secretion levels between plant-derived rGLP-1x10 incubated MIN6 cells and MIN6 cells incubated with GLP-1 standard (Figure 2.5A).

To verify that the observed increase in insulin secretion from MIN6 cells was induced by intact rGLP-1x10 decamer and not by its degradation products (such as the native GLP-1 monomer unit, known to be biologically active), following insulin secretion assays, cell-supernatants were subsequently assessed by 12.5% (w/v) SDS-PAGE and immunoblotting using anti-GLP-1 to observe the structural integrity of rGLP-1x10 following incubation. As shown in Figure 2.5B, a single band was detected (~36 kDa), indistinguishable in size from previously observed plant-derived rGLP-1x10 decamer,

Figure 2.5

Effect of tobacco-derived rGLP-1x10 protein on insulin secretion from MIN6 cells and subsequent rGLP-1x10 protein stability following incubation. (A) The mouse pancreatic beta-cell line MIN6, was incubated for 135 min with 10 mM glucose in DMEM in the presence of His-purified plant-derived rGLP-1x10 (250 ng/mL), GLP-1 standard (250 ng/mL), His-purified wild-type 81V9 TSP (250 ng/mL) or DMEM media. Insulin concentration from collected cell-supernatants was determined using an insulin ELISA kit (Crystal Chem Inc.) followed by reading of OD at 450 nm. Data shown represent averages in triplicate with error bars corresponding to standard deviation. (B) Culture supernatant of MIN6 cells were collected at different incubation times following treatment with His-purified plant-derived rGLP-1x10 and analyzed for rGLP-1x10 integrity by 12.5% (w/v) SDS-PAGE followed by Immunoblotting using anti-GLP-1 antibody. The arrow corresponds to the only detectable band corresponding to the expected size for rGLP-1x10 at all three time points, suggesting high stability of the GLP-1x10 protein. Coomassie blue staining of the blot following film development ensured equal loading.

A

Insulin stimulatory effect of plant-derived rGLP-1x10 on MIN6 cells *in vitro*

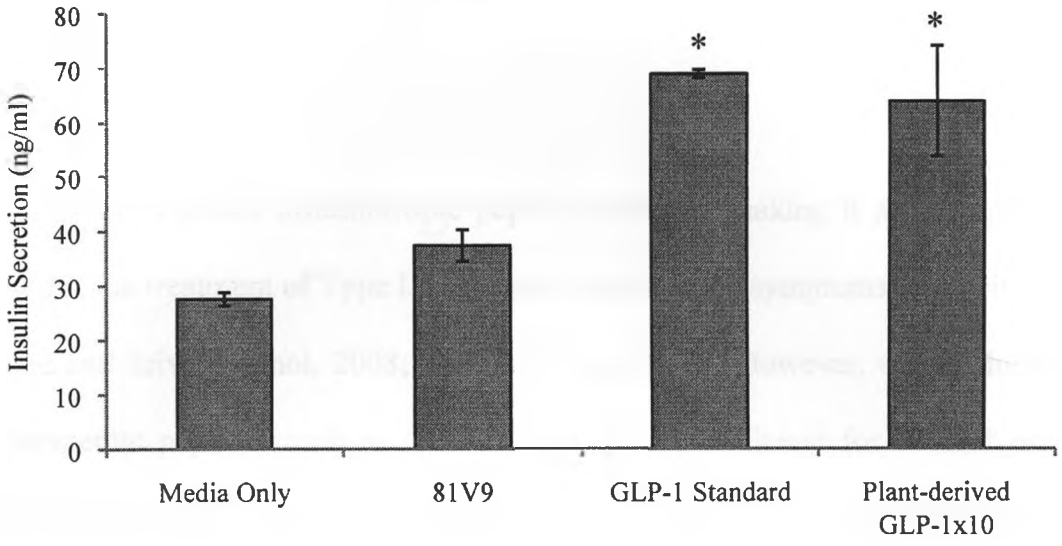

* $p < 0.05$

B

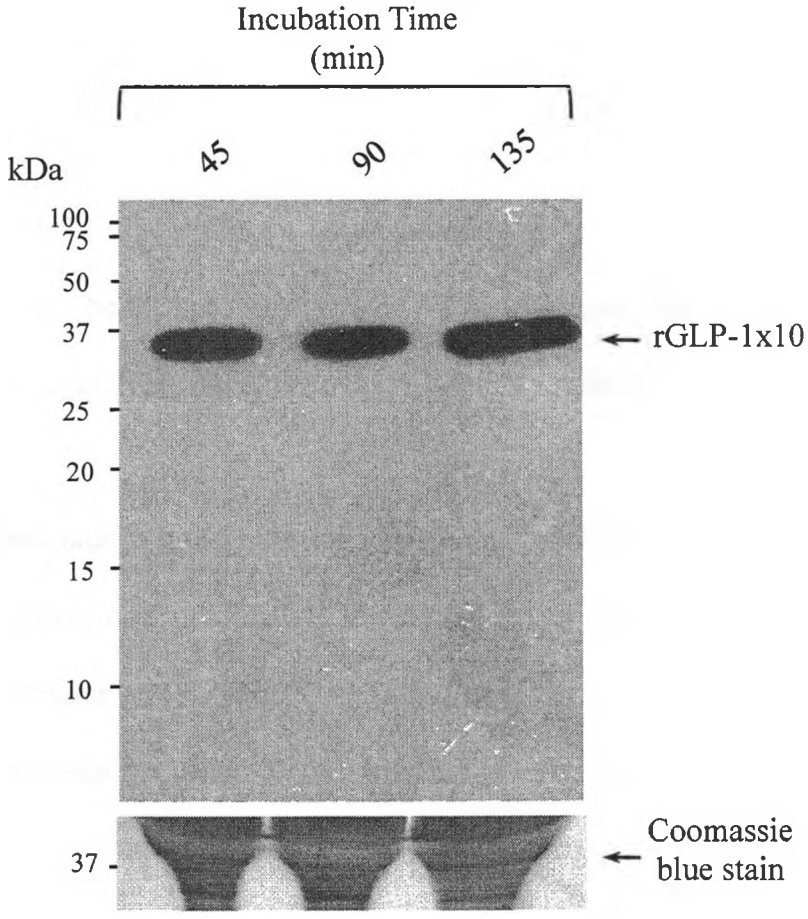

suggesting that no degradation of rGLP-1x10 occurred during incubation with MIN6 cells. Taken together, results suggest plant-derived rGLP-1x10 decamer is biologically active.

2.4 Discussion

GLP-1 is a potent insulinotropic peptide hormone, making it an attractive drug candidate for the treatment of Type II diabetes and its related symptoms (Gallwitz, 2005; Thongtang and Sriwijitkamol, 2008; Yu and Wang, 2008). However, the production of small therapeutic peptides such as GLP-1, in quantities sufficient for clinical use is a challenging task. Traditionally, chemical synthesis methods are used for the production of therapeutic peptides (Kimmerlin and Seebach, 2005). Despite its speed and efficiency, a major limitation of chemical synthesis is its low product yield. The use of recombinant DNA technology has the potential to overcome this limitation. Both bacterial and yeast expression systems have demonstrated the viable production of rGLP-1 (Chen *et al.*, 2007; Hou *et al.,* 2007a, b). Microbial-based production systems such as bacteria and yeast however, may not be the system of choice for large-scale manufacturing of rGLP-1 as their production capacity is dependent upon expensive fermentation equipment and infrastructure.

In the present study, transgenic tobacco plants were assessed as an alternative bioreactor for the production of rGLP-1. It was the intent of this research to express *GLP-1* as a large decamer protein (GLP-1x10), in hopes that this would increase protein stability and thus facilitate the accumulation of rGLP-1 in transgenic plants. Immunoblot analysis using anti-GLP-1 antibody confirmed the accumulation of a single protein band

of the expected size for a rGLP-1 decamer from tobacco plants transformed with pALP-GLP-1x10 (Figure 2.3B). Yasuda *et al.*, report that rGLP-1 pentamer could be accumulated in rice seed when fused to the signal peptide of rice glutelin, which directs protein to the endoplasmic reticulum (ER). However, the rice seed-derived recombinant protein is smaller in size than that calculated for a GLP-1 pentamer, and moreover, it was not demonstrated whether rGLP-1 pentamer is biologically active (Yasuda *et al.*, 2006). Previously, the production of rGLP-1 in both yeast and bacteria were demonstrated by expressing *GLP-1* as a large multimer comprised of ten or eight tandem repeats of *GLP-1* sequence respectively (Hou *et al.*, 2007a, b).

Taken together, results suggest that recombinant expression of GLP-1 can be optimized through multimerization. This technology has now been increasingly exploited as an effective and reliable tool for achieving efficient mass production of recombinant therapeutic peptides. For example, Tian *et al.*, reported high level accumulation of an antimicrobial peptide (bovine lactoferrin derivative LfcinB15-W410), in *E. coli* when it was expressed as a tetramer repeat. Kim *et al.*, found that the antimicrobial histonin peptide was accumulated at high levels in *E. coli* when it was expressed as a peptide multimer. In addition to improving the stability and consequently the accumulation of therapeutic peptides, multimerization may also improve the therapeutic potential of a peptide. Protein/peptide oligomerization may lead to functional advantages such as higher binding strengths, increased immunological potency, and the modification of *in vivo* pharmacokinetic properties (Steif *et al.*, 1993). It has been reported that multimerizing T cell epitopes increases the immunological potency of soluble peptides and can promote either antigen-specific T cell activation or tolerance through *in vitro*

activation-induced cell death at much lower concentrations than the native monomeric peptide (Falk *et al.*, 2000; Rotzschke *et al.*, 1997). Piaggio *et al.*, demonstrated intravenous injection of very low-doses of peptides made from multiple copies of the recognized pancreatic self-antigen epitope (multimerized T cell epitopes) prevented autoimmune diabetes in animal models by inducing dominant tolerance.

The accumulation level of plant-derived rGLP-1x10 was quantified using indirect ELISA (Figure 2.4). Due to the sequence repeat nature of synthetic *GLP-1x10*, quantification of rGLP-1x10 with ELISA using anti-GLP-1 antibody would confuse ELISA results, as anti-GLP-1 antibody contains the potential to bind a single GLP-1x10 protein a total of 10 times. If commercially available monomeric GLP-1 is to be used as an ELISA standard, signal intensities cannot be compared to experimental unknowns as anti-GLP-1 antibody could only ever bind the GLP-1 standard once. To alleviate this concern, an anti-6xHis-tag antibody was used for ELISA, as the 6xHis-tag was present in only a single sequence motif on each plant-derived rGLP-1x10 protein. For this ELISA, a standard curve was generated from a 6xHis-tag-containing reference protein of known quantity. Indirect ELISA results indicate that plant-derived recombinant GLP-1x10 accumulates up to 0.15% of tobacco plant TSP (Figure 2.4). This is an encouraging accumulation level, suggesting that the rGLP-1 multimer is quite stable in transgenic tobacco.

The biological activity of the plant-derived rGLP-1x10 was determined by its ability to stimulate insulin secretion from a mouse pancreatic beta-cell line (MIN6) *in vitro*. The MIN6 cell line is derived from a transgenic mouse expressing the large T-antigen of SV40 in pancreatic beta-cells, and exhibits characteristics of glucose

metabolism and glucose-stimulated insulin secretion similar to those of normal islets (Miyazaki *et al.*, 1990). MIN6 cells have been used extensively as an *in vitro* model to study the mechanism of glucose-stimulated insulin secretion in pancreatic beta-cells. Data collected in this study indicate insulin concentration in MIN6 cell-supernatant collected after 135 min incubation in the presence of 6xHis-purified plant-derived rGLP-1x10, is comparable to that detected in cell-supernatant from MIN6 cells incubated with commercial GLP-1 standard (Figure 2.5A). More importantly, insulin concentrations in MIN6 cell-supernatant incubated with 6xHis-purified plant-derived rGLP-1x10 is significantly ($p<0.05$) higher than those from MIN6 cell-supernatant incubated with 6xHis-purified wild-type 81V9 TSP or media only (Figure 2.5A).

To assess whether plant-derived rGLP-1x10 remained intact after stimulation of insulin secretion, MIN6 cell-supernatant incubated with plant-derived rGLP-1x10 was subsequently analyzed for the presence of rGLP-1x10 by SDS-PAGE and immunoblotting. Immunoblot analysis using anti-GLP-1 antibody confirmed a single band corresponding in size (~36 kDa) to that of a GLP-1 decamer (Figure 2.5B). Together, these data strongly suggest that plant-derived rGLP-1x10 in its synthetic decamer form is biologically active. It is believed this study is the first to report the ability of rGLP-1 to retain insulin-stimulatory activity *in vitro* while contained within a multimer structure. Although rGLP-1 multimers containing variable numbers of *GLP-1* repeat have been previously produced using different expression platforms, their biological activity was always demonstrated following enzymatic cleavage of the rGLP-1 multimer into its native monomeric form (Hou *et al.*, 2007a, b; Sugita *et al.*, 2005; Yasuda *et al.*, 2005, 2006). This study indicates it is not necessary to convert rGLP-1

multimers to native GLP-1 monomer constituents to obtain biological activity. This finding will help improve GLP-1 production efficiency and reduce overall GLP-1 production cost due to reduced RTP processing. Furthermore, the lack of detectable rGLP-1x10 degradation (Figure 2.5B) suggests plant-derived rGLP-1 decamer is stable *in vitro*, a feature that may help increase its therapeutic potency if oral administration is attempted.

In summary, a new approach for the production of rGLP-1 in transgenic tobacco plants, based on the use of DNA fusion techniques to construct a synthetic gene expressing *GLP-1* as a tandem-repeat decamer, has been developed. The data indicate plant-derived rGLP-1x10 is stably accumulated in tobacco plants transformed with pALP-GLP-1x10, and that the plant-derived recombinant protein retains its native biological activity to stimulate insulin secretion from MIN6 cells *in vitro* while remaining in its synthetic decamer form. This is the first demonstration of the generation of transgenic tobacco accumulating rGLP-1 as a decamer protein. Furthermore, this report is the first to demonstrate the biological activity of rGLP-1 while still retained as a multimer protein and not as its native monomer peptide *in vitro*.

2.5 References

Bevan, M. (1984). Binary *Agrobacterium* vectors for plant transformation. Nucleic Acids Res. *12,* 8711-8721.

Boehm, R. (2007). Bioproduction of therapeutic proteins in the 21st century and the role of plants and plant cells as production platforms. Ann. N. Y. Acad. Sci. *1102,* 121-134.

Bulotta, A., Farilla, L., Hui, H., and Perfetti, R. (2004). The role of GLP-1 in the regulation of islet cell mass. Cell Biochem. Biophys. *40,* 65-78.

Carrington, J.C., and Freed, D.D. (1990). Cap-independent enhancement of translation by a plant potyvirus 5' nontranslated region. J. Virol. *64,* 1590-1597.

Chen, J., Bai, G., Cao, Y., Gao, Z., Zhang, Q., Zhu, Y., and Yang, W. (2007). One-step purification of a fusion protein of glucagon-like peptide-1 and human serum albumin expressed in *Pichia pastoris* by an immunomagnetic separation technique. Biosci. Biotechnol. Biochem. *71,* 2655-2662.

Daniell, H. (2006). Production of biopharmaceuticals and vaccines in plants via the chloroplast genome. Biotechnol. J. *1,* 1071-1079.

Drucker, D.J. (2003). Enhancing incretin action for the treatment of type 2 diabetes. Diabetes Care *26,* 2929-2940.

Edwards, C.M. (2005). The GLP-1 system as a therapeutic target. Ann. Med. *37,* 314-322.

Edwards, C.M., Todd, J.F., Ghatei, M.A., and Bloom, S.R. (1998). Subcutaneous glucagon-like peptide-1 (7-36) amide is insulinotropic and can cause hypoglycaemia in fasted healthy subjects. Clin. Sci. (Lond) *95,* 719-724.

Falk, K., Rotzschke, O., and Strominger, J.L. (2000). Antigen-specific elimination of T cells induced by oligomerized hemagglutinin (HA) 306-318. Eur. J. Immunol. *30,* 3012-3020.

Gallwitz, B. (2005). Glucagon-like peptide-1-based therapies for the treatment of type 2 diabetes mellitus. Treat. Endocrinol. *4,* 361-370.

Holst, J.J. (2007). The physiology of glucagon-like peptide 1. Physiol. Rev. *87,* 1409-1439.

Horsch R.B., Fry J.E., Hoffmann N.L., Eicholtz D., Rogers S.G., and Fraley R.T. (1985). A simple and general method for transferring genes into plants. Science *227,* 1229-1231.

Hou, J., Yan, R., Ding, D., Yang, L., Wang, C., Wu, Z., Yu, X., Li, W., and Li, M. (2007a). Oral administration of a fusion protein containing eight GLP-1 analogues produced in *Escherichia coli* BL21(DE3) in streptozotocin-induced diabetic rats. Biotechnol. Lett. *29,* 1439-1446.

Hou, J., Yan, R., Yang, L., Wu, Z., Wang, C., Ding, D., Li, N., Ma, C., and Li, M. (2007b). High-level expression of fusion protein containing 10 tandem repeated GLP-1 analogs in yeast *Pichia pastoris* and its biological activity in a diabetic rat model. Biosci. Biotechnol. Biochem. *71,* 1462-1469.

Kim, J.M., Jang, S.A., Yu, B.J., Sung, B.H., Cho, J.H., and Kim, S.C. (2008). High-level expression of an antimicrobial peptide histonin as a natural form by multimerization and furin-mediated cleavage. Appl. Microbiol. Biotechnol. *78,* 123-130.

Kimmerlin, T., and Seebach, D. (2005). '100 Years of peptide synthesis': ligation methods for peptide and protein synthesis with applications to beta-peptide assemblies. J. Pept. Res. *65,* 229-260.

Latham, P.W. (1999). Therapeutic peptides revisited. Nat. Biotechnol. *17,* 755-757.

Ma, S., Huang, Y., Davis, A., Yin, Z., Mi, Q., Menassa, R., Brandle, J.E., and Jevnikar, A. (2005). Production of biologically active human interleukin-4 in transgenic tobacco and potato. Plant Biotech. J. *3,* 309-318.

Miyazaki, J., Araki, K., Yamato, E., Ikegami, H., Asano, T., Shibasaki, Y., Oka, Y., and Yamamura, K. (1990). Establishment of a pancreatic beta cell line that retains glucose-inducible insulin secretion: special reference to expression of glucose transporter isoforms. Endocrinology *127,* 126-132.

Nathan, D.M., Schreiber, E., Fogel, H., Mojsov, S., and Habener, J.F. (1992). Insulinotropic action of glucagonlike peptide-I-(7-37) in diabetic and nondiabetic subjects. Diabetes Care *15,* 270-276.

Nauck, M.A., Heimesaat, M.M., Orskov, C., Holst, J.J., Ebert, R., and Creutzfeldt, W. (1993). Preserved incretin activity of glucagon-like peptide 1 (7-36 amide) but not of synthetic human gastric inhibitory polypeptide in patients with type-2 diabetes mellitus. J. Clin. Invest. *91,* 301-307.

Piaggio, E., Mars, L.T., Cassan, C., Cabarrocas, J., Hofstatter, M., Desbois, S., Bergereau, E., Rotzschke, O., Falk, K., and Liblau, R.S. (2007). Multimerized T cell epitopes protect from experimental autoimmune diabetes by inducing dominant tolerance. Proc. Natl. Acad. Sci. U. S. A. *104,* 9393-9398.

Rotzschke, O., Falk, K., and Strominger, J.L. (1997). Superactivation of an immune response triggered by oligomerized T cell epitopes. Proc. Natl. Acad. Sci. U. S. A. *94,* 14642-14647.

Schillberg, S., Twyman, R.M., and Fischer, R. (2005). Opportunities for recombinant antigen and antibody expression in transgenic plants-technology assessment. Vaccine *23,* 1764-1769.

Steif, C., Weber, P., Hinz, H.J., Flossdorf, J., Cesareni, G., and Kokkinidis, M. (1993). Subunit interactions provide a significant contribution to the stability of the dimeric four-alpha-helical-bundle protein ROP. Biochemistry *32,* 3867-3876.

Sugita, K., Endo-Kasahara, S., Tada, Y., Lijun, Y., Yasuda, H., Hayashi, Y., Jomori, T., Ebinuma, H., and Takaiwa, F. (2005). Genetically modified rice seeds accumulating GLP-1 analogue stimulate insulin secretion from a mouse pancreatic beta-cell line. FEBS Lett. *579,* 1085-1088.

Thongtang, N., and Sriwijitkamol, A. (2008). Incretins: the novel therapy of type 2 diabetes. J. Med. Assoc. Thai. *91,* 943-954.

Tian, Z.G., Teng, D., Yang, Y.L., Luo, J., Feng, X.J., Fan, Y., Zhang, F., and Wang, J.H. (2007). Multimerization and fusion expression of bovine lactoferricin derivative LfcinB15-W4,10 in *Escherichia coli.* Appl. Microbiol. Biotechnol. *75,* 117-124.

Wang, D.J., Brandsma, M., Yin, Z., Wang, A., Jevnikar, A.M., and Ma, S. (2008). A novel platform for biologically active recombinant human interleukin-13 production. Plant. Biotechnol. J. *6,* 504-515.

Wise, A.A., Liu, Z., and Binns, A.N. (2006). Three methods for the introduction of foreign DNA into *Agrobacterium.* Methods Mol. Biol. *343,* 43-53.

Yasuda, H., Hayashi, Y., Jomori, T., and Takaiwa, F. (2006). The correlation between expression and localization of a foreign gene product in rice endosperm. Plant Cell Physiol. *47,* 756-763.

Yasuda, H., Tada, Y., Hayashi, Y., Jomori, T., and Takaiwa, F. (2005). Expression of the small peptide GLP-1 in transgenic plants. Transgenic Res. *14,* 677-684.

Yu, B.S., and Wang, A.R. (2008). Glucagon-like peptide 1 based therapy for type 2 diabetes. World J. Pediatr. *4,* 8-13.

Chapter 3

An innovative approach for the production of multi-use human serum transferrin

---

3.1 Introduction

The Tf family of proteins comprises a diverse class of homologous iron-binding proteins found in all vertebrates (Harris and Aisen, 1989), whose major function surrounds iron sequestration and transport. Most of the members of the Tf class are monomeric glycoproteins with a glycosylation-dependent molecular mass in the range of 76-81 kDa, each consisting of two structurally similar, but not identical polypeptide lobes and a single short connecting peptide (Huebers and Finch, 1987). Each Tf lobe contains a single iron-binding site such that one Tf molecule can carry a maximum of two iron atoms (Huebers and Finch, 1987). The hsTf protein consists of 679 amino acids containing two *N*-linked glycan chains attached to Asn residues at positions 413 and 611, with a calculated (glycosylated) molecular mass of 79.5 kDa (Huebers and Finch, 1987). The hsTf protein is synthesized predominantly in the liver and is secreted into the blood plasma for transport of iron throughout the body. Endogenously, hsTf exists in either holo- (iron bound) or apo-hsTf (iron free) forms. In addition to its well-documented iron transport function, hsTf may also have other biological activities. For example, hsTf has been identified as a major growth factor involved in promoting the clonal growth of

murine granulocyte and macrophage precursors cultured *in vitro* under serum-free conditions (Iizuka and Murphy, 1986), and has shown to be vital for most mammalian cells to grow in culture, such as *in vitro* fertilization cultures (Holst *et al.*, 1990), and in the maintenance and expansion of stem cell populations (Furue *et al.*, 2008). Furthermore, hsTf also has a synergistic effect with other growth factors such as epidermal growth factor (Briere *et al.*, 1991) and insulin (Watkins *et al.*, 1990) to stimulate eukaryotic cell growth. In addition, hsTf has been shown to delay bacterial and fungal growth, most likely through the binding of iron in solution, resulting in reduced iron availability required for microbial growth (Artis *et al.*, 1983; Salamah and Al-Obaidi, 1995)

The multifunctional nature of hsTf can be exploited for a variety of practical applications. Many serum-free medium formulations developed to support mammalian cell culture growth contain hsTf as a serum substitute (Barnes and Sato, 1980). The hsTf protein has also actively been applied as a bacteriostatic agent, reducing the further propagation of both bacteria and fungi both *in vitro* and *in vivo* (Bullen *et al.*, 1978; Bullen, 1981; Ellison *et al.*, 1988). Recently, hsTf has attracted a great deal of attention as a transport chaperone for fused therapeutics, intended for enhanced therapeutic transport across the blood-brain barrier (Friden and Walus, 1993; Osborn *et al.*, 2008) to target tumor cells (Liu *et al.*, 2009; Nakase *et al.*, 2008) or to enhance therapeutic bioavailability upon oral delivery of protein and peptide drugs (Bai *et al.*, 2005; Widera *et al.*, 2003, 2004). However, applications for hsTf often require the availability of large amounts of functional hsTf at affordable cost, necessitating the development of a highly efficient and cost-effective expression platform for production of rhsTf.

Production of rhsTf has been reported in several expression systems. The accumulation of rhsTf in *E. coli* resulted in only inactivated products, largely due to incorrect intramolecular disulphide bond formation (de Smit *et al.*, 1995; Ikeda *et al.*, 1992; Steinlein and Ikeda, 1993). The hsTf protein has a complex molecular structure and its biological activity largely depends on the correct formation of all 19 intramolecular disulfide bonds (MacGillivray *et al.*, 1998). As an alternative to bacterial production, a BHK cell-based expression system was developed for rhsTf production as well as rhsTf glycosylation-defective mutants (Funk *et al.*, 1990; Mason *et al.*, 1991, 1993, 2001, 2004). Although viable, BHK cell-based rhsTf production is limited by low product yield. To alleviate rhsTf production limitations, other expression systems have been investigated, including yeast (Mason *et al.*, 1996; Sargent *et al.*, 2006), *Drosophila* S2 cells (Lim *et al.*, 2004) and other insect cell lines (Ali *et al.*, 1996). Although each of these bioreactors has its own inherent benefits for rhsTf production, each also has its own limitations. All current platforms for rhsTf production are cell culture-based expression systems, making it difficult and expensive to scale up the manufacture of rhsTf to commercial volumes due to inherent dependencies on expensive growth media and fermentation equipment. As a result, the plant bioreactor may prove to be a suitable alternative to microbial and cell-based methods for rhsTf generation due to its many inherent production benefits as outlined in section 1.2.3.

The following describes an investigation of the feasibility of using transgenic plants as a novel bioreactor for the production of rhsTf. Since native hsTf is a secreted molecule, rhsTf was targeted to the ER in transgenic tobacco plants for improved accumulation. Results presented here demonstrate that transgenic tobacco plants can

accumulate rhsTf at relatively high levels. Further biochemical and functional characterization of rhsTf shows plant-derived rhsTf, although nonglycosylated as judged by an enzymatic deglycosylation analysis, displays many of the native functions of hsTf *in vitro*. In particular, plant-derived rhsTf reversibly binds iron, delays the growth of pathogenic bacteria, and promotes the proliferation of mammalian cells all *in vitro*. Results described here suggest plant-derived rhsTf may have numerous commercial and therapeutic applications, thereby supporting the use of transgenic plants as a novel source for the generation of functional rhsTf.

3.2 Materials and Methods

3.2.1 Plant expression vector construction

A 2094 bp cDNA encoding *hsTf* as well its native signal peptide (Accn. #NM_001063) was purchased from OriGene ((Cat. #RC209184) Rockville, MD, USA) within the pCMV6 Entry vector.* The coding region of *hsTf* was amplified from pCMV6 by PCR using designed forward primer TF1 (5'-ATGATATC**ATG**AGGCTCGC CGTGGGAGC-3') and reverse primer TF2 (5'-AA**TCTAGA**TTA*AAGCTCATCCTT*AT GATGATGATGATGATGAGGTCTACGGAAAGTGCAGGC-3'). Primer TF1 incorporates an *Eco*RV restriction site (underlined) immediately upstream of a start codon (bold). Primer TF2 contains an engineered *Xba*I restriction site (bold) immediately downstream of a stop codon (double underlined), an ER retention signal KDEL (italic) and a hexahistidine purification tag (underlined). PCR amplifications were performed

---

* For further information regarding bacterial strains, plasmid extraction, ligation and bacterial transformation procedures, refer to Appendix 1.

using a PCR Sprint Thermal Cycler (Thermo Fischer Scientific Inc., Waltham, MD, USA) under the following parameters: denature at 94°C for 45 s, anneal at 55°C for 45 s and elongate at 72°C for 2 min, for a total of 35 cycles, followed by a final elongation at 72°C for 10 min. The PCR product was blunt-end ligated into the *Hinc*II restriction site of pUC19 (Accn. #L09137) to generate plasmid pUC19-hsTf and was subsequently sequenced to confirm *hsTf* sequence integrity (Sequencing Facility, Robarts Research Institute, London, ON). The *hsTf* coding region was released from pUC19-hsTf as an *Eco*RV/*Xba*I fragment and ligated into pBlueUTL* at *Xba*I/*Sma*I restriction sites to generate plasmid pUTL-hsTf. The *UTL-hsTf* sequence was released from pUTL-hsTf as an *Xho*I/*Xba*I fragment and ligated into pRTL-GUS (Carrington and Freed, 1990) by replacement of *UTL-GUS*, generating plasmid pRTL-hsTf. Plasmid pRTL-GUS includes the constitutive double 35S promoter of the CaMV in tandem and the *NOS* terminator sequence. The 3' *Xba*I restriction site of *hsTf* in pRTL-hsTf was destroyed by digestion with *Xba*I, treatment with Klenow fragment (Fermentas, Glen Burnie, MD, USA), and subsequent blunt-end ligation. The *hsTf* expression cassette was removed from pRTL-hsTf as an *Sph*I fragment, blunt-ended by treatment with Klenow fragment and inserted into pBluescript II SK(-) (Fermentas) at *Sma*I, generating pBlu35S-hsTf. The entire *hsTf* expression cassette was removed from pBlu35S-hsTf as a *Sal*I/*Xba*I fragment for subsequent cloning into the binary plant transformation vector pBIN19 (Bevan, 1984), to generate the final plant transformation vector pRJC-hsTf.

---

* pBlueUTL is derived from pBluescript II SK(-) (Accn. #X52329) and contains a cloned TEV 5' UTL released from pRTL-GUS (Carrington and Freed, 1990) as an *Eco*RI/*Nco*I fragment, with *Nco*I restriction site destroyed by Klenow and subsequent ligation to pBluescript II SK(-) at *Eco*RI and *Sma*I restriction sites.

3.2.2 Generation of transgenic plants

Tobacco plants transformed with pRJC-hsTf were generated in the identical method as is described in section 2.2.2 for the generation of tobacco accumulating rGLP-1x10.

3.2.3 Screening of putative transgenic plants by PCR and RT-PCR

Total gDNA was extracted from tobacco plants transformed with pRJC-hsTf using a basic phenol/chloroform method. For further detail on this extraction procedure, refer to Appendix 1.8. Previously described primers (TF1 and TF2) were used to probe extracted tobacco gDNA for the presence of *hsTf* using identical PCR parameters and cycler described in the generation of the *hsTf* expression cassette in section 3.2.1. The same described conditions and primer pairs were used to assess gDNA extracted from untransformed 81V9 control tobacco plants. All PCR products were separated by electrophoresis on a 0.75% (w/v) agarose gel and analyzed by UV visualization using ethidium bromide staining.

For RT-PCR analysis, total RNA was extracted from putative transgenic plants as described in section 2.2.3. Approximately 150 ng of first-strand synthesized tobacco plant cDNA was used as a template for PCR amplification in a 100 µl reaction volume using identical conditions and primers (TF1 and TF2) outlined above for the detection of tobacco genome-integrated *hsTf*. PCR reactions using identical conditions and primers on extracted tobacco RNA samples without first-strand cDNA synthesis were used as negative controls. All RT-PCR samples were subsequently separated by electrophoresis

on a 0.75% (w/v) agarose gel and analyzed by UV visualization using ethidium bromide staining.

3.2.4 Immunoblot analysis

Only transgenic tobacco plants confirmed by PCR for genomic *hsTf* insertion and accumulation of *hsTf* transcripts by RT-PCR were analyzed by SDS-PAGE followed by immunoblotting to confirm the accumulation of rhsTf in transgenic plants. Transgenic tobacco TSP was extracted from tobacco-leaf tissue as described in section 2.2.4. The concentration of extracted TSP was determined by the method of Bradford using Bio-Rad protein assay dye reagent and BSA (Sigma-Aldrich) as a protein standard. Extracted tobacco TSP samples and commercial hsTf standard (Sigma-Aldrich) were boiled for 10 min in sample buffer [63 mM Tris-HCl, 2% (w/v) SDS, 10% (v/v) glycerol, 0.1 M DTT, 0.01% (w/v) bromophenol blue, pH 6.8] and separated on 12.5% (w/v) SDS-PAGE gels. Gels were transferred to PVDF membranes (Millipore, Burlington, MA, USA) using a semi-dry transfer method and blocked for 1 h in 5% (w/v) skim milk-TBST [20 mM Tris, 150 mM NaCl, 0.02% (v/v) Tween-20, pH 7.6]. Blots were incubated at room temperature for 2 h with goat anti-hsTf monoclonal primary antibody (Sigma-Aldrich) diluted to 1:500 (v/v) in 1.7% (w/v) skim milk-TBST. Following TBST washes, swine anti-goat IgG secondary antibody conjugated with horseradish peroxidase (Amersham Pharmacia Biotech) was added for 1 h at room temperature. Protein band detection on each blot was achieved using the ECL reaction kit (Amersham Pharmacia Biotech) according to the manufacturer's instructions.

3.2.5 ELISA quantification of plant-derived rhsTf

Recombinant hsTf protein accumulated in transgenic tobacco plants was quantified using an indirect Enzyme Linked ImmunoSorbent Assay (ELISA) compared against known quantities of hsTf reference protein (Sigma-Aldrich). Total protein samples extracted as described in section 3.2.4, were resuspended in sodium bicarbonate (pH 9.6), coated onto a 96-well mictrotiter plate, and incubated overnight at 4°C. Wells were washed three times with PBST [phosphate buffered saline containing 0.05% (v/v) Tween-20] and blocked with 3% (w/v) BSA in PBST for 2 h at room temperature. After washing with PBST, goat anti-hsTf monoclonal antibody (Sigma-Aldrich) diluted to 1:5000 (v/v) was added to plates and incubated overnight at 4°C. After three subsequent PBST washes, horseradish peroxidase-conjugated swine anti-goat IgG antibody (Amersham Pharmacia Biotech) was added at a 1:2000 (v/v) dilution and incubated at room temperature for 1 h. Enzyme substrate TMB (R&D Systems) was added to each well (as per the manufacturer's instructions) and the plate was incubated at room temperature in the dark for 30 min. The reaction was stopped with addition of 100 μL/well stop solution (R&D Systems). The absorbance was measured at 450 nm in a microplate reader (Bio-Rad 3550), and converted as a percentage of tobacco TSP by reference to an ELISA standard curve constructed with commercially available hsTf standard (Sigma-Aldrich).

3.2.6 Purification of His-tagged rhsTf

Plant-derived rhsTf was purified from transgenic tobacco TSP leaf extracts of tobacco plants transformed with pRJC-hsTf using histidine affinity chromatography as described for rGLP-1x10 purification in section 2.2.6.

3.2.7 Enzymatic deglycosylation

Plant-derived rhsTf was assessed for any associated *N*-linked glycans using Peptide N-glycosidase F (PNGase F) (Sigma-Aldrich) digestion followed by SDS-PAGE and immunoblotting. Plant TSP extracts obtained from transgenic tobacco plants positive for the presence of rhsTf as determined by immunoblotting, as well as His-purified plant-derived rhsTf, were used for enzymatic digestions as per the manufacturer's instructions, overnight at 37°C. Commercially available glycosylated hsTf standard (Sigma-Aldrich) was used as a positive control. Prior to enzymatic digestion, all samples were denatured by boiling for 10 min in the presence of denaturing buffer [20 mM Na_2HPO_4 (pH 7.2), 1% (w/v) SDS, 0.5 M β-mercaptoethanol]. After enzymatic treatment, samples were analyzed by 12.5% (w/v) SDS-PAGE followed by immunoblotting using anti-hsTf monoclonal antibody (Sigma-Aldrich).

3.2.8 *In vitro* iron-binding assay

The ability of plant-derived rhsTf to bind iron *in vitro* was assessed using spectrophotometry by the method of Lim *et al.*, with minor modifications. Briefly, holo-rhsTf was generated using 5 mg of plant-derived His-purified or hsTf standard (Sigma-Aldrich) added to a solution containing excess of 25 μM $Fe(NTA)_2$. Apo-hsTf

solutions were prepared by addition of His-purified plant-derived rhsTf or hsTf standard (5 mg) to equal volumes of 100 mM sodium acetate and 1 mM EDTA at pH 4.0 for 30 min on ice, followed by extensive dialysis against PBS. Apo- or holo-hsTf solutions were incubated for 1 h at room temperature and their absorbance measured at 465 and 280 nm following a 1:10 (v/v) dilution. Iron-binding capacities of hsTf were expressed as a ratio of A_{465} / A_{280} with fully active hsTf having an A_{465} / A_{280} value of 0.048-0.050 (Bezkorovainy and Grohlich, 1970). Albumin protein from bovine serum (BSA, 5 mg) as well as His-purified wild-type 81V9 TSP (5 mg), were used as negative controls following apo- or holo-saturation treatment.

3.2.9 *Pseudomonas syringae* growth assay

Plant virulent *Pseudomonas syringae* pv *syringae* was grown overnight to an OD_{600} of approximately 0.7 and subcultured to fresh TB medium [12 g/L tryptone, 24 g/L yeast extract, 4 mL glycerol, pH 7.4] to a final dilution of 1:500 (v/v). After addition of equal volumes of TB medium, His-purified plant-derived apo-rhsTf (100 μg/mL), hsTf standard (100 μg/mL), or His-purified 81V9 TSP (100 μg/mL) to *P. syringae* samples, an initial OD_{600} reading was taken and determined as time 0. Readings of OD_{600} were taken every 3 h until the growth plateau was observed. Cultures of *P. syringae* (13 mL) were grown in 50 mL Falcon Conical tubes (BD Bioscience, San Jose, CA, USA) in a 37°C incubator, shaking at 250 rpm.

3.2.10 HeLa cell growth assay

The mammalian epithelial carcinoma cell-line HeLa 229 (ATCC, CCL-2.1) was maintained in RPMI 1640 medium (Sigma-Aldrich) supplemented with 10% (v/v) fetal calf serum, 100 U/mL penicillin, 0.1 mg/mL streptomycin, and 2 mM L-glutamine at 37°C in humidified incubators in an atmosphere of 5% CO_2 and 95% air. To determine the effect of plant-derived rhsTf on mammalian cell proliferation, cultured HeLa cells were harvested with Trypsin-EDTA solution (Sigma-Aldrich), centrifuged (1,500 rpm for 5 min), and washed with serum-free Ham's F12 medium (SFF12) (Hutchings and Sato, 1978) containing soybean trypsin inhibitor. Cells were then plated in tissue culture dishes (60x15 mm) at a density of ~$5x10^4$ cells per dish as determined by counting on a hemocytometer. Cultures were first incubated at 37°C for 30 min followed by addition of His-purified plant-derived rhsTf (50 μg/mL) or His-purified 81V9 TSP (50 μg/mL) in both apo- and holo-forms. An equal volume of SFF12 media only was used as a negative control with all cultures subsequently incubated for various time periods (1 to 4 days). Following incubation, the cells were trypsinized and counted in triplicate with a hemocytometer.

3.2.11 Assay for plant-derived rhsTf interaction to HeLa cells *in vitro*

To determine if plant-derived rhsTf is able to interact with mammalian HeLa cells *in vitro*, HeLa cells used to determine the effect of plant-derived rhsTf on cell growth as described in section 3.2.10 were collected and washed three times with ice-cold PBS to remove any unbound protein followed by treatment with lysis buffer [200 mM NaCl, 25 mM Tris-HCl, 5 mM imidazole, 0.1% (v/v) Triton X-100, pH 8.0]. Protein lysate was

separated by 12.5% (w/v) SDS-PAGE and Immunoblotted with anti-hsTf antibody (Sigma-Aldrich).

3.3 Results

3.3.1 Construction of expression vector and generation of transgenic plants

The plant expression vector pRJC-hsTf was generated for stable nuclear tobacco plant transformation and subsequent expression of *hsTf* under strong constitutive control of the CaMV 35S promoter in tandem as illustrated in Figure 3.1. The 5' UTL sequence derived from TEV RNA was incorporated into pRJC-hsTf with the intent to maximize *hsTf* expression (Gallie *et al.*, 1995). A 30 bp native hsTf signal peptide was incorporated on the N-terminus of the recombinant protein as well as ER-retention KDEL signal, located on the C-terminus, intended to maximize rhsTf accumulation (Ma *et al.*, 2005). A C-terminal 6xHis tag was included on pRJC-hsTf to facilitate downstream purification of rhsTf via IMAC.

Plant leaf-disc transformation was performed using *A. tumefaciens* containing pRJC-hsTf. A total of 25 independent transgenic tobacco plant lines were generated, with all transgenic plants showing normal growth and development and no phenotypic variance from standard untransformed wild-type 81V9 controls. Confirmation of *hsTf* integration into the tobacco plant nuclear genome was obtained by PCR using *hsTf* gene-specific primers (TF1 and TF2), generating a single band corresponding in size (2124 bp) to that of *hsTf* (Figure 3.2A). No PCR product was obtained using identical primers and reaction conditions from gDNA prepared from untransformed wild-type 81V9 tobacco plants (Figure 3.2A).

Figure 3.1

Plant expression vector pRJC-hsTf. Plant binary transformation vector pRJC-hsTf: LB – left border, P_{NOS} – nopaline synthase promoter, NPT-II – neomycin phosphotransferase II marker, T_{NOS} – nopaline synthase terminator, CaMV 35S x 2 –constitutive cauliflower mosaic virus 35S promoter in tandem, TEV – tobacco etch virus UTL sequence, hsTf – coding region of human serum transferrin, KDEL – ER retention signal, 6xHis – C-terminal His-purification tag, RB – right border. Note: diagram is not drawn to scale.

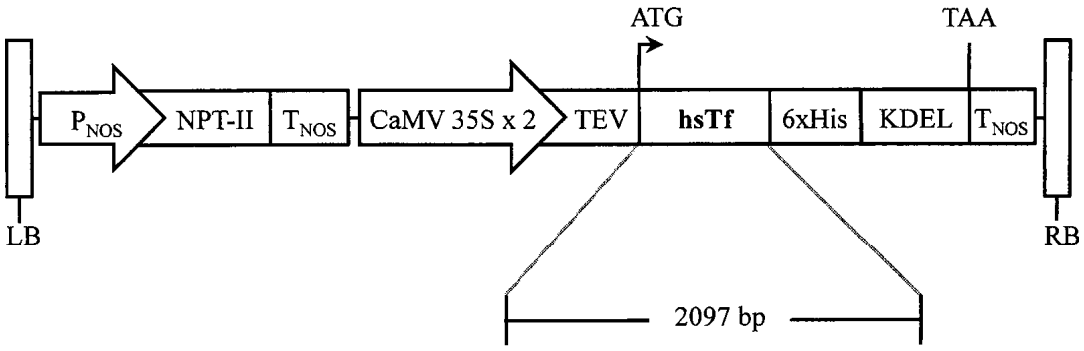
ATG
TAA
LB
P_{NOS}
NPT-II
T_{NOS}
CaMV 35S x 2
TEV
hsTf
6xHis
KDEL
T_{NOS}
RB
2097 bp

Figure 3.2

PCR and RT-PCR analysis of transgenic hsTf tobacco plants. (A) Total gDNA was extracted from putative transgenic tobacco plants transformed with pRJC-hsTf. The resulting gDNA was used for PCR amplification using Taq polymerase and primers TF1 and TF2 to yield a single product of identical size to that of *hsTf*: pUC19-TF – positive pDNA control, 81V9 – untransformed wild-type tobacco control, TF2-TF14 – independent transgenic tobacco lines transformed with pRJC-hsTf. (B) Detection of *hsTf* mRNA in transgenic tobacco plants transformed with pRJC-hsTf by RT-PCR. Total RNA was extracted from putative transgenic tobacco plants and converted to cDNA. A total of 150 ng of cDNA was used for PCR amplification using Taq polymerase and primers TF1 and TF2 to generate a single product corresponding in size to *hsTf*. The quality of cDNA was confirmed by PCR analysis using *actin* specific primers (see Table 2 for sequence). The arrows correspond to bands of interest. The numerical values to the left represent the size in base pairs (bp) of the DNA marker. All samples were separated by electrophoresis on 0.75% (w/v) agarose gels followed by UV visualization using ethidium bromide staining.

A

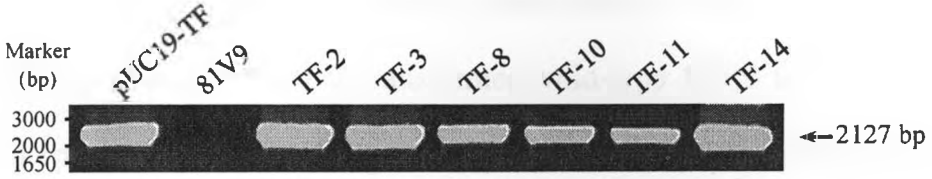
Marker
(bp)
pUC19-TF
81V9
TF-2
TF-3
TF-8
TF-10
TF-11
TF-14
3000
2000
1650
2127 bp

B

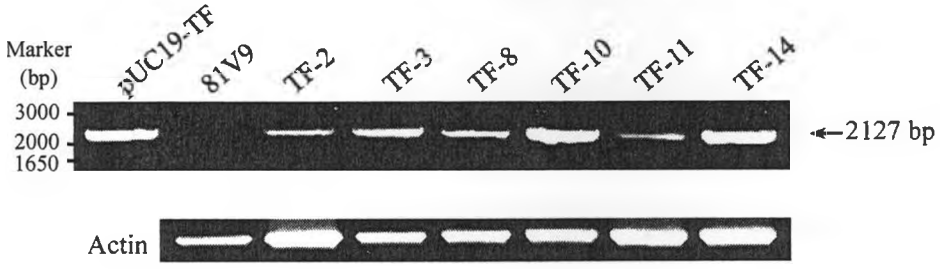
Marker
(bp)
pUC19-TF
81V9
TF-2
TF-3
TF-8
TF-10
TF-11
TF-14
3000
2000
1650
2127 bp
Actin

3.3.2 *hsTf* transcripts accumulate in transgenic plants

Independent transgenic tobacco plant lines transformed with pRJC-hsTf and confirmed positive for *hsTf* nuclear integration by PCR were analyzed for detection of *hsTf* transcripts by RT-PCR. Primers specific for *hsTf* (TF1 and TF2) were used to generate a product of expected size (2124 bp) from prepared cDNA samples (Figure 3.2B). No RT-PCR product was obtained using identical primers and reaction conditions from cDNA prepared from untransformed wild-type 81V9 tobacco plants. PCR amplification was performed on all RNA samples without first strand synthesis to rule out possible amplification of contaminant DNA in the samples. No amplified PCR product was generated using this method, eliminating the possibility of DNA contamination of extracted RNA samples (data not shown). Detection of *actin* transcripts in extracted RNA samples using *actin*-specific primers was used as a positive control to ensure the quality of generated cDNA (Figure 3.2B, Table 2)

3.3.3 rhsTf accumulates in transgenic plants

The accumulation of rhsTf in transgenic tobacco plants transformed with pRJC-hsTf was examined by immunoblotting using anti-hsTf monoclonal antibody (Sigma-Aldrich). Total protein extracts were obtained from tobacco plants positive for the detection of *hsTf* transcripts by RT-PCR. As shown in Figure 3.3A, anti-hsTf antibodies detected a single band from transgenic tobacco plant TSP samples corresponding in size to the ~76.5 kDa hsTf standard. No bands were detected from TSP extracted from untransformed 81V9 control plants (Figure 3.3A). The relative accumulated amount of rhsTf in transgenic tobacco plant TSP extracts was measured

Figure 3.3

Immunoblot analysis of tobacco-derived rhsTf protein and its quantification by indirect ELISA. (A) Total soluble protein (TSP) extracted from tobacco transformed with pRJC-hsTf and standardized to 45 μg was separated by 12.5% (w/v) SDS-PAGE, transferred onto PVDF membrane, and probed with anti-hsTf. The arrow labeled rhsTf corresponds to the recombinant protein of interest: PC –hsTf standard, 81V9 – untransformed wild-type tobacco control, TF8-TF20 independent tobacco lines transformed with pRJC-hsTf. The numerical values to the left refer to the size in kilo Daltons of the protein marker. Following film development, blot (A) was stained with coomassie blue to ensure equal loading. (B) TSP extracted from leaves of tobacco transformed with pRJC-hsTf was used to estimate the relative accumulation level of plant-derived rhsTf using indirect ELISA as described in section 3.2.7: TF2-TF20 – independent transgenic tobacco lines transformed with pRJC-hsTf. The data represent averages of three independent experiments. Error bars correspond to standard deviation.

A

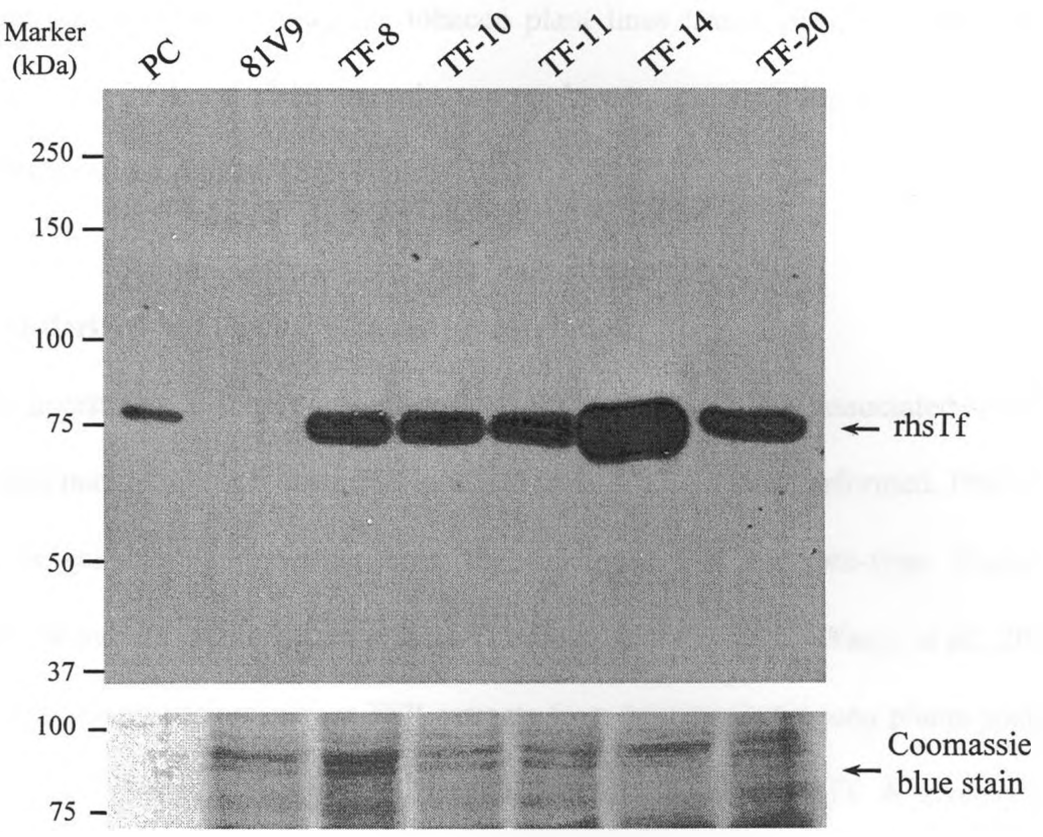
Marker
(kDa)
PC
81V9
TF-8
TF-10
TF-11
TF-14
TF-20
250
150
100
75
50
37
rhsTf
100
75
Coomassie
blue stain

B

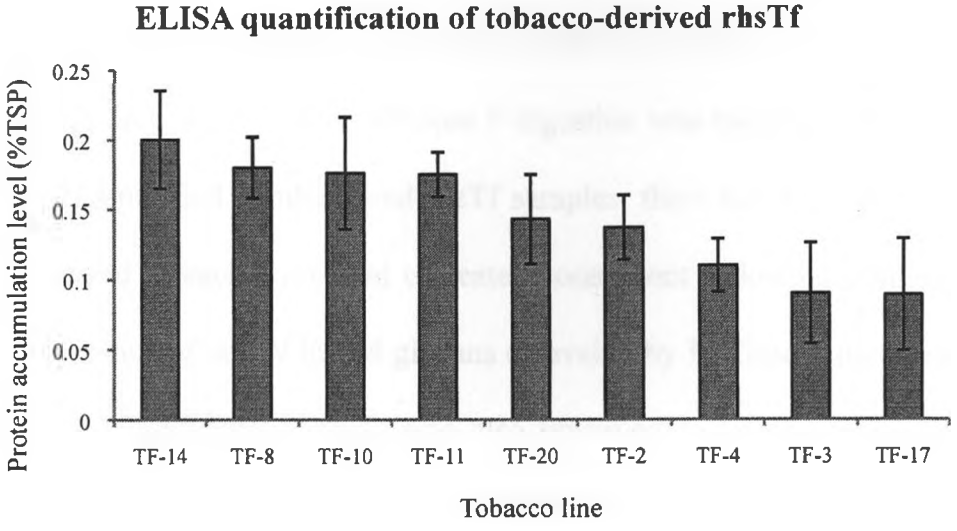
ELISA quantification of tobacco-derived rhsTf
Protein accumulation level (%TSP)
0.25
0.2
0.15
0.1
0.05
0
TF-14
TF-8
TF-10
TF-11
TF-20
TF-2
TF-4
TF-3
TF-17
Tobacco line

using an indirect ELISA method with anti-hsTf antibody (Sigma-Aldrich) and compared against a hsTf standard (Sigma-Aldrich). Accumulation levels of rhsTf were found variable among individual transgenic tobacco plant lines transformed with pRJC-hsTf. Plant lines TF14, TF8 and TF10 were the top producers, accumulating rhsTf at levels of nearly 0.2% of tobacco plant TSP (Figure 3.3B).

3.3.4 Plant-derived hsTf lacks *N*-linked glycosylation

To investigate if tobacco plant-derived rhsTf contained any associated *N*-linked glycans, enzymatic digestion using PNGase F (Sigma-Aldrich) was performed. PNGase F digestion is capable of removing both high-mannose and complex-type *N*-glycans commonly found on plant glycoproteins (Lerouge *et al.*, 1998, Wang *et al.*, 2008). Samples were obtained from either TSP extracts from transgenic tobacco plants positive for rhsTf accumulation or samples of His-purified plant-derived rhsTf. A glycosylated hsTf standard (Sigma-Aldrich) was used as a positive control. Following treatment with PNGase F and subsequent SDS-PAGE and immunoblotting, commercially available hsTf standard migrated just below its untreated constituent indicating the presence of *N*-linked glycans (Figure 3.4). Furthermorethe PNGase F-treated hsTf standard shows the presence of no other bands, indicating that the PNGase F digestion was specific and complete. For both TSP and His-purified plant-derived rhsTf samples, there was no detection of band migration compared to each correlated untreated constituent following immunoblotting, indicating the absence of any *N*-linked glycans cleavable by PNGase F digestion (Figure 3.4). The tobacco plant-derived rhsTf was also observed to be of similar size to the glycosylated hsTf standard (Figure 3.4), most likely indicating incorrect processing of the

Figure 3.4

Deglycosylation assay of tobacco-derived rhsTf. Enzymatic digestion of hsTf with PNGase F was performed overnight at 37°C followed by 12.5% (w/v) SDS-PAGE and immunoblotting using anti-hsTf: PC –hsTf standard, hsTf TSP – total soluble protein sample of plant-derived rhsTf, His-purified hsTf – plant-derived His-purified rhsTf, "-" – untreated sample, "+" – treated sample. Arrows indicate the gel mobility shift of the hsTf standard. Numerical values on the left refer to the size in kilo Daltons of the protein marker.

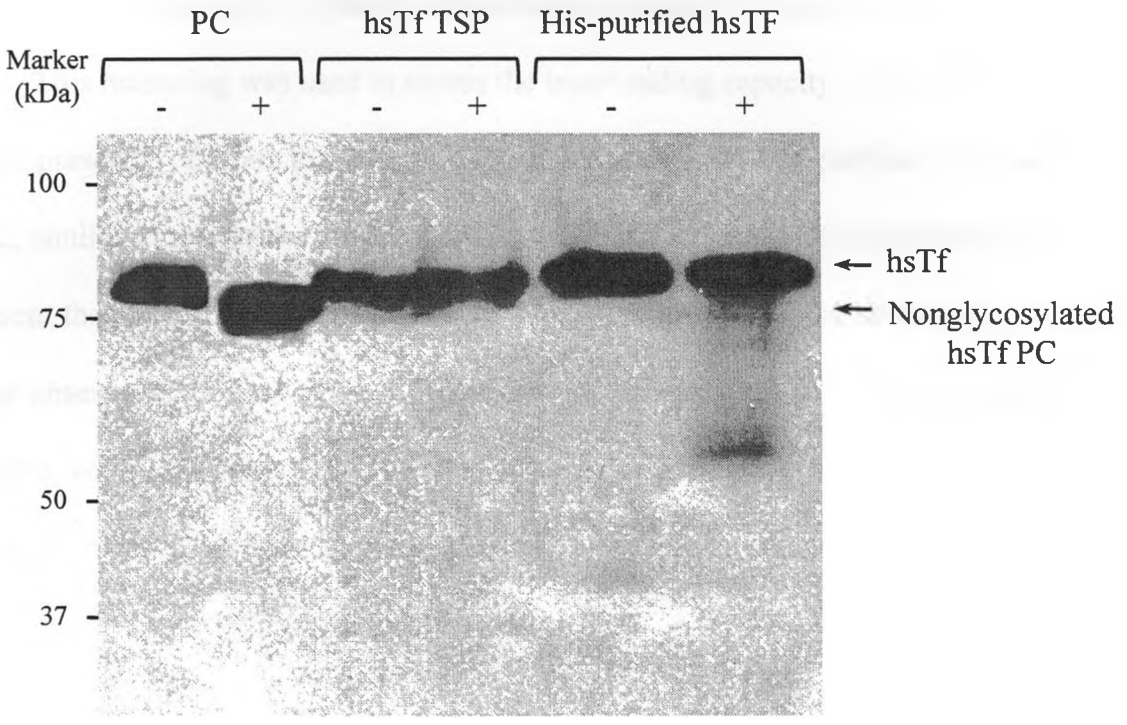
PC
hsTf TSP
His-purified hsTF
Marker
(kDa)
-
+
-
+
-
+
100
75
50
37
hsTf
Nonglycosylated
hsTf PC

native signal peptide as well as addition of KDEL and 6xHis tag, contributing to an additional possible 30 amino acids (~3.5 kDa).

3.3.5 Plant-derived rhsTf reversibly binds iron *in vitro*

Fully active, holo-hsTf has a well-documented A_{465} / A_{280} of 0.048-0.05, significantly different from values derived from apo-hsTf (Bezkorovainy and Grohlich, 1970). This reasoning was used to assess the iron-binding capacity of plant-derived rhsTf. In the presence of iron, the A_{465} / A_{280} of plant-derived His-purified holo-rhsTf was 0.052, similar to that of the human-derived holo-hsTf standard and significantly ($p<0.05$) different then negative controls (Table 1). Absorbance values were subsequently reduced in the absence of iron and lower pH, and were insignificant ($p>0.05$) compared to the negative controls (Table 1). The non-related protein BSA as well as His-purified wild-type 81V9 TSP samples were used as negative controls, showing no change in A_{465} / A_{280} values with the addition of iron.

3.3.6 Plant-derived rhsTf delays pathogenic bacterial growth

Plant-derived rhsTf was assessed *in vitro* for any effect in the delay of growth of the gram-negative plant pathogen *P. syringae*. Measurements of OD_{600} were used to assess the cell density of *P. syringae* samples every 3 h. As shown in Figure 3.5, *P. syringae* growth was not completely inhibited compared to negative controls, but was significantly delayed ($p<0.05$) upon administration of His-purified plant-derived apo-rhsTf in solution. Commercially available apo-hsTf standard (Sigma-Aldrich) was used as a positive control and displayed similar bacteriostatic effects to plant-derived

Table 1. Iron-binding Activity of Plant-derived rhsTf

	Fe^{3+}				No Fe^{3+}			
	Apo-hsTf (Human)	Apo-hsTf (Plant)	Apo-81V9	BSA	Apo-hsTf (Human)	Apo-hsTf (Plant)	Apo-81V9	BSA
A_{465} / A_{280}	0.051*	0.052*	0.018	0.017	0.015	0.017	0.016	0.018

* $p<0.05$

rhsTf on *P. syringae* growth. A His-purified TSP sample of wild-type 81V9 was used as a negative control and showed insignificant ($p>0.05$) effects on *P. syringae* growth compared to that of TB medium only (Figure 3.5).

3.3.7 Plant-derived rhsTf stimulates mammalian cell growth

The ability to stimulate the immortal mammalian HeLa cell-line with His-purified plant-derived holo-rhsTf allowed further characterization of the biological activity of the plant-derived recombinant protein. HeLa cells were grown to a density of ~$5x10^4$ cells/dish and administered plant-derived His-purified holo-rhsTf, His-purified holo-81V9 negative control, or serum-free medium only. Cell growth was assessed daily by counting on a hemocytometer in triplicate. As shown in Figure 3.6A, plant-derived holo-rhsTf significantly ($p<0.05$) enhanced mammalian HeLa cell growth *in vitro* when administered in solution over a 4-day period, compared to negative controls. Both plant-derived apo-rhsTf and His-purified 81V9 TSP (administered apo-treatment) were also assessed for their effects on HeLa cell growth *in vitro* and were shown to have insignificant ($p>0.05$) effects (data not shown).

To determine if plant-derived rhsTf is able to interact with mammalian HeLa cells *in vitro* either through cell-surface binding or cellular internalization, HeLa cells administered plant-derived holo-rhsTf for growth assessment were subsequently collected and extensively washed with PBS before being lysed. The protein lysate was assessed for the presence of rhsTf by immunoblotting using anti-hsTf. As shown in Figure 3.6B, only HeLa cell-samples administered apo- or holo-rhsTf contained detectable levels of rhsTf after immunoblotting, indicating that plant-derived rhsTf interacts with mammalian HeLa

Figure 3.5

Effect of tobacco-derived rhsTf on bacterial growth. His-purified plant-derived apo-rhsTf was assessed for its effect against the growth of the plant pathogen *P. syringae* as described in section 3.2.9. A significant ($p<0.05$) delay in *P. syringae* growth was observed, as assessed by measurements of OD_{600} following the addition of plant-derived apo-rhsTf at 12 and 15 hours post rhsTf inoculation. The bacteriostatic effect of plant-derived hsTf was shown to be similar to that of the hsTf standard (PC). The His-purified wild-type 81V9 control had no significant effect on *P. syringae* growth compared to bacterial growth in medium only. Eventually (24 hours post hsTf inoculation) all samples reached a similar cell density as determined by OD_{600}.

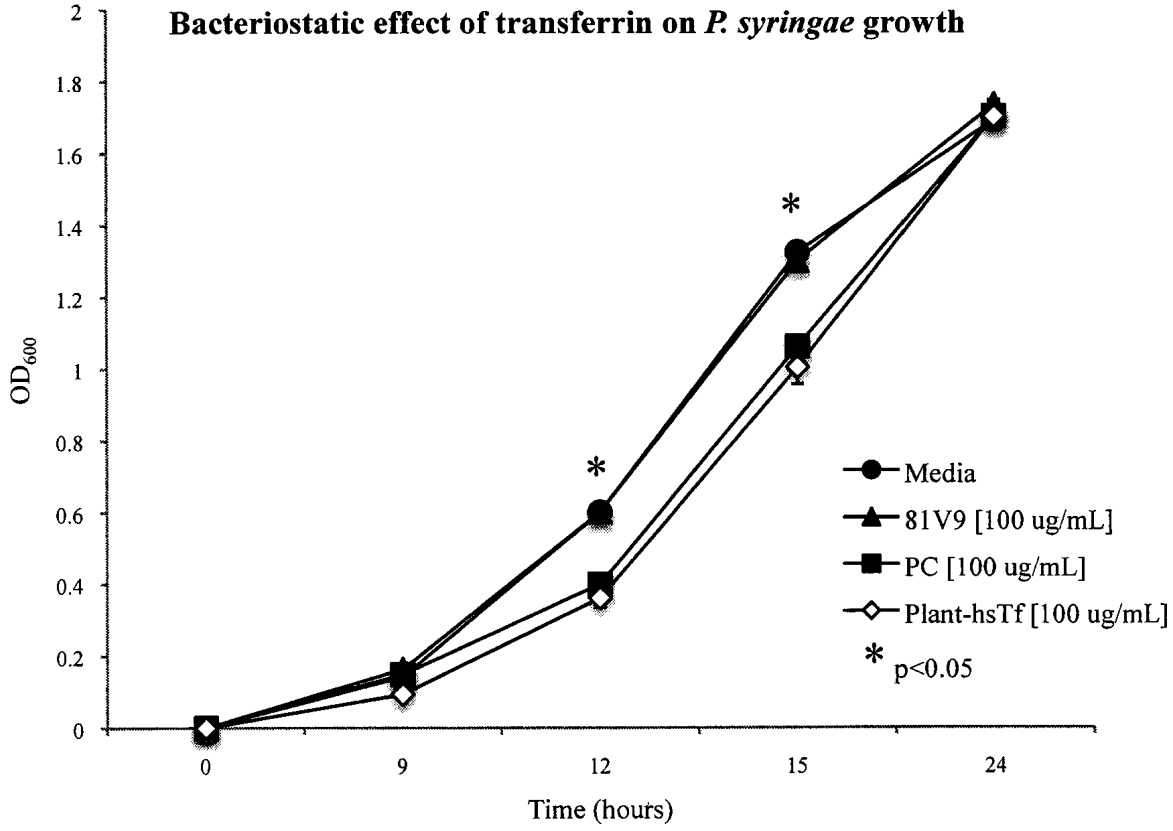
Bacteriostatic effect of transferrin on P. syringae growth
OD600
2
1.8
1.6
1.4
1.2
1
0.8
0.6
0.4
0.2
0
0
9
12
15
24
Time (hours)
*
*
Media
81V9 [100 ug/mL]
PC [100 ug/mL]
Plant-hsTf [100 ug/mL]
* p<0.05

Figure 3.6

Effect of tobacco-derived rhsTf on mammalian cell growth. (A) His-purified plant-derived holo-rhsTf was assessed for its ability to stimulate the growth of the mammalian immortal HeLa cell line as described in section 3.2.10. A significant ($p<0.05$) increase in HeLa cell growth was observed following the addition of (50 μg/mL) His-purified plant-derived holo-rhsTf (F12 + Tf) after 4 and 5-days of incubation. The His-purified wild-type 81V9 (50 μg/mL) control (F12 + 81V9) had an insignificant effect on HeLa cell growth compared to HeLa cell growth in serum-free media only (F12). (B) HeLa cells used to determine the effect of plant-derived rhsTf on cell growth were collected, extensively washed with PBS, and lysed to determine if plant-derived rhsTf interacts with HeLa cells *in vitro*. The protein lysate was separated by 12.5% (w/v) SDS-PAGE, transferred to PVDF and analyzed by immunoblotting using anti-hsTf. The arrow labeled rhsTf corresponds to the recombinant protein of interest. HeLa cell samples were administered serum-free F12 medium only (Media), His-purified untransformed holo- or apo-81V9 (Holo-81V9, Apo-81V9), or His-purified plant-derived rhsTf administered holo-(Holo-hsTf (plant)) or apo-(Apo-hsTf (plant)) treatment in the concentrations noted above. Following film development, blot (B) was stained with coomassie blue to ensure equal loading. All numerical values on the left refer to the size in kilo Daltons of the protein marker.

A

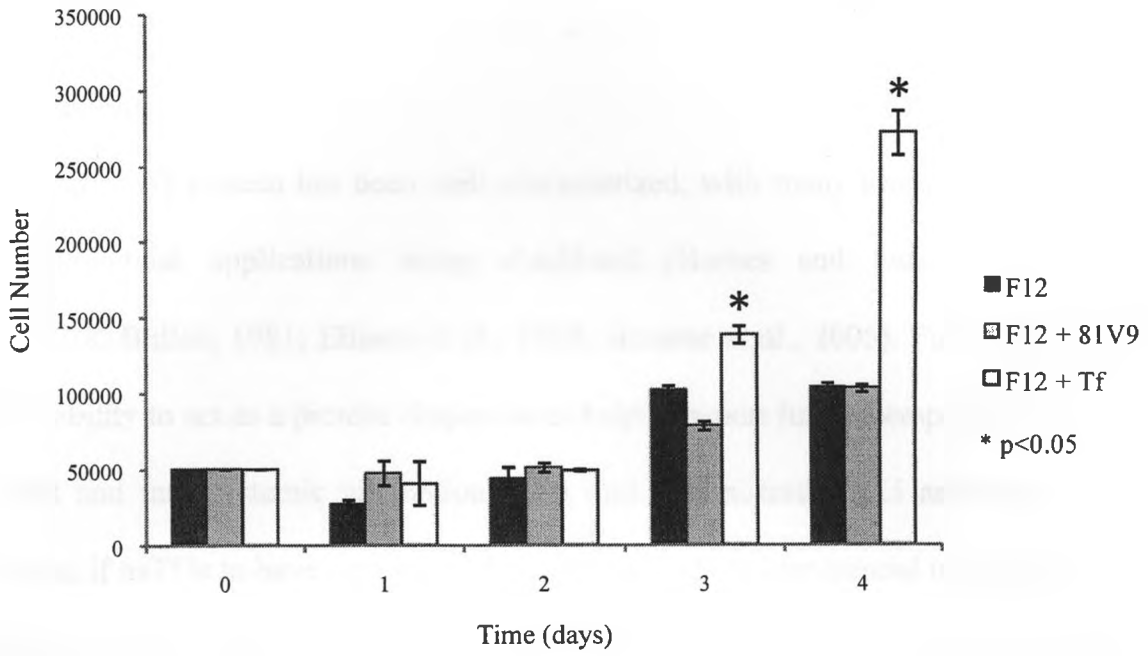
Effect of plant-derived rhsTf on HeLa cell growth
Cell Number
350000
300000
250000
200000
150000
100000
50000
0
0
1
2
3
4
Time (days)
*
*
F12
F12 + 81V9
F12 + Tf
* p<0.05

B

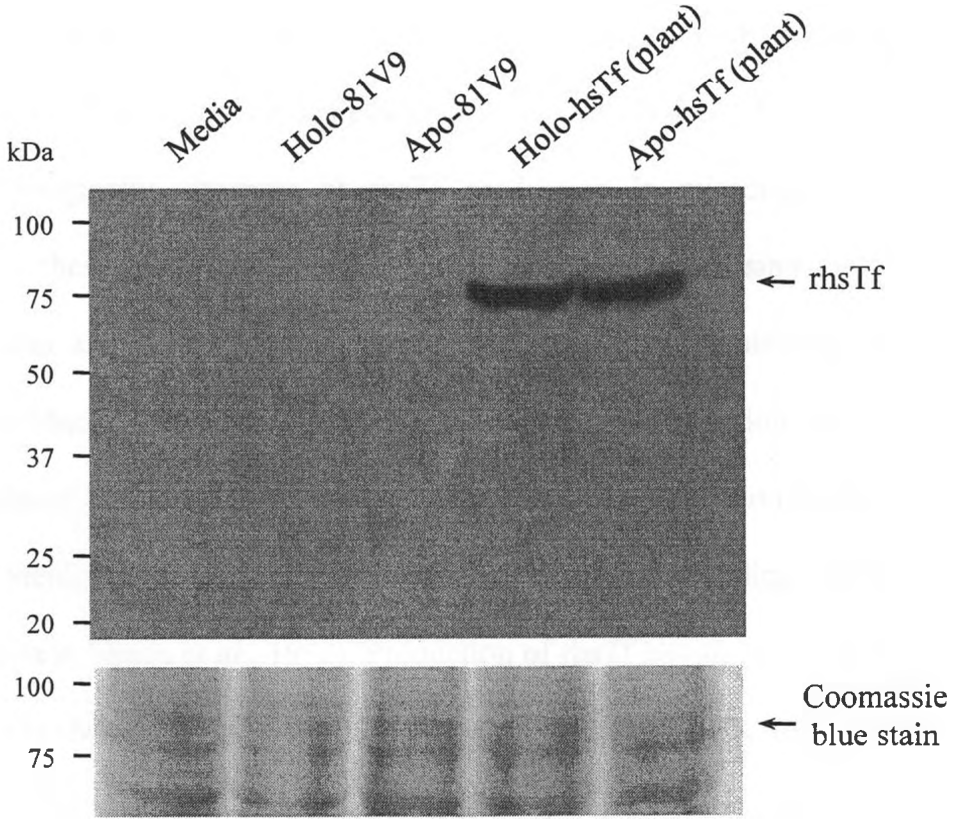
kDa
Media
Holo-81V9
Apo-81V9
Holo-hsTf (plant)
Apo-hsTf (plant)
100
75
50
37
25
20
rhsTf
100
75
Coomassie blue stain

cells *in vitro*. No hsTf was detected in cell samples administered apo- or holo-81V9 TSP or serum-free media only following immunoblotting (Figure 3.6B).

3.4 Discussion

The hsTf protein has been well characterized, with many associated therapeutic and commercial applications being elucidated (Barnes and Sato, 1980; Bullen *et al.*, 1978; Bullen, 1981; Ellison *et al.*, 1988; Gomme *et al.*, 2005). Furthermore, hsTf has the ability to act as a protein chaperone to help transport fused therapeutics out of the GI tract and into systemic circulation upon oral administration (Li and Qian, 2002). However, if hsTf is to have significant future therapeutic or commercial use, efficient and economical production of rhsTf must be achieved. Recombinant DNA technology has the potential to generate large amounts of RTPs of interest both efficiently and economically. Bacterial and yeast expression platforms have been generated with the intent to produce functional rhsTf (de Smit *et al.*, 1995; Funk *et al.*, 1990; Ikeda *et al.*, 1992; Steinlein and Ikeda, 1993). Originally, attempts at rhsTf production in microbial hosts proved unsuccessful, as these platforms were thought incapable of processing the large hsTf (~76 kDa) protein and its inherent intramolecular complexity, containing 19 internal disulfide bonds (MacGillivray *et al.*, 1998). In addition, rhsTf expression in *E. coli* results in the accumulation of recombinant product within insoluble inclusion bodies, severely limiting rhsTf yield, and demonstrating no evidence of the iron-binding potential of the recombinant protein (Ikeda *et al.*, 1992). Production of rhsTf has also been demonstrated within BHK cells (Mason *et al.*, 1993, 2001, 2004). Although BHK cell-derived rhsTf can reversibly bind iron *in vitro*, this bioreactor generates relatively low yield of

recombinant product while adding to increased cost and production complications associated with eukaryotic cell culture systems. It is apparent microbial and cell culture-based fermentation of rhsTf may not be suitable for the production of commercial volumes of rhsTf.

In the present study, transgenic plants were assessed as an alternative system for the production of rhsTf. It was the intent of this research to express *hsTf* in transgenic tobacco plants with the hope of providing a novel bioreactor for rhsTf production that could surmount current bioreactor limitations. Immunoblot analysis using anti-hsTf antibody confirmed the accumulation of a single protein band of the expected size (~76 kDa) for hsTf (Figure 3.3A). Furthermore, data gained from indirect ELISA results indicate that plant-derived rhsTf accumulates up to 0.2% of tobacco plant TSP (Figure 3.3B). This is the first study to report accumulation of rhsTf in any plant host.

The hsTf protein contains two internal *N*-linked glycosylation sites located at the carboxy-terminal domain (Asn_{413} and Asn_{611}) of the protein (MacGillivray *et al.*, 1983). To assess whether plant-derived rhsTf contained associated *N*-linked glycans, PNGase F digestion of both His-purified and non-purified plant-derived rhsTf was performed and subsequently analyzed by SDS-PAGE and immunoblotting. PNGase F digestion is capable of removing both high-mannose and complex-type *N*-glycans commonly found on plant glycoproteins (Lerouge *et al.*, 1998, Wang *et al.*, 2008). Results here indicate that plant-derived rhsTf contains no associated *N*-linked glycans cleavable by PNGase F digestion, as a gel mobility shift was not observed following PNGase F digestion and subsequent immunoblotting (Figure 3.4). Commercially available, glycosylated hsTf standard (Sigma-Aldrich) was also assessed with PNGase F digestion. Following

digestion and subsequent analysis by SDS-PAGE and immunoblotting, a single band-shift was observed for the hsTf standard, confirming the integrity and specificity of the reaction (Figure 3.4). Analysis also shows that the plant-derived rhsTf migrates to the similar size of glycosylated hsTf standard, even though it most likely contains no associated glycans cleavable by PNGase F digestion (Figure 3.4). The apparent additional molecular mass of plant-derived rhsTf may be attributed to ineffective processing of its native signal peptide as well as incorporation of KDEL and 6xHis purification tag, accounting for a possible 30 additional amino acids (~3.5 kDa).

Previous reports indicate that not all potential sites of *N*-glycosylation are necessarily occupied, as occupancy depends on many factors including host type, stress, and growth conditions (Yet and Wold, 1990). Indeed, recombinant interleukin-10 (IL-10) containing a single potential glycosylation site as well as native signal peptide and KDEL sequence, was shown to have no associated glycans when accumulated in a plant host (Menassa *et al.*, 2007). Both glycosylated and non-glycosylated versions of rhsTf derived from BHK cells were assessed for receptor binding affinity and were shown to have no variance, indicating that associated carbohydrates have no role in hsTf receptor binding and subsequent function (Mason *et al.*, 1993). In a similar study, N- and C-terminal half-rhsTf proteins were produced in *E. coli*, with only *N*-linked glycosylation associated with the C-lobe (Hoefkens *et al.*, 1996). Upon assessment in receptor binding affinity, data indicated each rhsTf lobe had no significant variation for receptor affinity (Hoefkens *et al.*, 1996). Furthermore, glycosylation may only have a possible role in hsTf receptor function (Byrne *et al.*, 2006). Although the function of *N*-linked hsTf glycosylation remains unknown, results do suggest hsTf associated glycans may play a role in the

redistribution of iron in cases of iron deficiency (de Jong *et al.*, 1990). The potential lack of associated glycans to plant-derived rhsTf is not believed to limit the commercial or therapeutic use of tobacco plant-derived rhsTf.

It has been previously reported that fully active and completely saturated hsTf has an A_{465} / A_{280} value of 0.048-0.050 (Bezkorovainy and Grohlich, 1970). Results here indicate that A_{465} / A_{280} value of plant-derived rhsTf in the presence of iron are significantly ($p<0.05$) different than negative controls *in vitro* and similar ($p>0.05$) to that of an hsTf standard (Table 1). These findings provide further evidence that associated *N*-linked glycans are not necessary in the sequestering of iron in solution by hsTf. Similar results were also shown with the production of unglycosylated rhsTf in *Drosophila* S2 cells (Lim *et al.*, 2004).

Much research has demonstrated the inhibitory effect of hsTf and its associated constituents such as lactoferrin on the growth of gram-negative bacteria (Bullen *et al.*, 1978; Ellison *et al.*, 1988). Human pathogenic species of *Pseudomonas* are only able to survive in mammalian serum because they are able to produce siderophores that can out-compete hsTf for iron acquisition within sera and allow for subsequent *Pseudomonas* growth within the blood (Ankenbauer *et al.*, 1985). Results from this study confirmed that plant-derived apo-rhsTf is able to delay significantly ($p<0.05$) *in vitro* growth of the pathogenic plant bacterium *P. syringae* (Figure 3.5). As hsTf is simply a bacteriostatic (not bacteriocidal) agent, limiting microbial growth due to iron saturation (Moore *et al.*, 1980), once all the rhsTf in a solution has been saturated, microbial growth can resume. This is apparent in this study as all *P. syringae* samples, with or without apo-rhsTf administration, eventually reached similar cell densities (Figure 3.5). This is

believed to be the first report of rhsTf affecting the growth of a known plant pathogen. Studies expressing lactoferrin in both transgenic rice and plant-cell culture have indeed shown a similar inhibitory effect against many plant pathogens including *P. syringae* (Mitra and Zhang, 1994; Takase *et al.*, 2005). In addition, data collected from rice-derived lactoferrin accumulation indicate that recombinant lactoferrin is able to defend against pathogenic attack *in planta*. These results suggest that plant-derived rhsTf may be able to perform a similar function, signifying hsTf expression as a potentially novel method of crop resistance to pathogenic bacteria.

To assess the further potential application of plant-derived rhsTf, His-purified plant-derived holo-rhsTf was administered to mammalian HeLa cells in a serum-free medium and observed for its effect on cell growth. Data collected here indicate that the presence of plant-derived His-purified holo-rhsTf in serum-free media significantly ($p<0.05$) increases the growth of mammalian HeLa cells *in vitro* over a 4-day period (Figure 3.6A). Commercial applications for rhsTf as an additive in serum-free media have indeed been marketed under the product name of DeltaFerrin™ (Keenan *et al.*, 2006). Traditionally, a plasma-derived hsTf analogue from an animal host is used as a growth factor in mammalian cell growth media. More recently, animal-free biopharmaceutical production has been noted as a gold standard, as this eliminates possible mammalian-viral contamination. As plant-derived rhsTf is shown to retain mammalian cell-growth stimulation effects, it too may represent an alternative source for rhsTf for applications involved in the manufacture of mammalian cell-growth media.

Plant-derived rhsTf was assessed for possible physical interaction with mammalian HeLa cells *in vitro*. HeLa cells used in growth assays were subsequently

collected and extensively washed to remove any non-bound proteins. After lysing the cells, the total protein lysate was analyzed by SDS-PAGE and immunoblotting to detect for the presence of hsTf using anti-hsTf antibody. As shown in Figure 3.6B, only HeLa cell samples administered plant-derived rhsTf (apo- or holo-) contained detectable amounts of hsTf. As HeLa cells could indeed contain endogenous hsTf, HeLa cells administered medium only or His-purified 81V9 TSP were also analyzed for the presence of hsTf, with no detectable levels observed (Figure 3.6B). Taken together, data here suggest that plant-derived rhsTf is able to interact with mammalian HeLa cells, either with cell-surface binding and/or cellular internalization. As plant-derived hsTf appears to retain native receptor binding abilities, it suggests the recombinant protein may make an excellent transport chaperone for other therapeutics.

In summary, a novel approach for the production of rhsTf in transgenic tobacco plants, based on the use of recombinant DNA strategies, has been developed. Plant-derived rhsTf is stably accumulated in transgenic tobacco transformed with pRJC-hsTf and that plant-derived rhsTf is non-glycosylated. Data also suggest that although plant-derived rhsTf lacks detectable *N*-linked glycosylation, it retains its native biological function to bind iron reversibly *in vitro*. Further assays indicate that plant-derived rhsTf is able to stimulate mammalian cell growth when added to serum-free medium as well as delay plant pathogenic bacterium growth *in vitro*. This is the first demonstration of rhsTf being successfully accumulated in transgenic plants with many of its native biological functions intact.

3.5 References

Ali, S.A., Joao, H.C., Csonga, R., Hammerschmid, F., and Steinkasserer, A. (1996). High-yield production of functionally active human serum transferrin using a baculovirus expression system, and its structural characterization. Biochem. J. *319,* 191-195.

Ankenbauer, R., Sriyosachati, S., and Cox, C.D. (1985). Effects of siderophores on the growth of *Pseudomonas aeruginosa* in human serum and transferrin. Infect. Immun. *49,* 132-140.

Artis, W.M., Patrusky, E., Rastinejad, F., and Duncan, R.L. Jr. (1983). Fungistatic mechanism of human transferrin for *Rhizopus oryzae* and *Trichophyton mentagrophytes*: alternative to simple iron deprivation. Infect. Immun. *41,* 1269-1278.

Bai, Y., Ann, D.K., and Shen, W.C. (2005). Recombinant granulocyte colony-stimulating factor-transferrin fusion protein as an oral myelopoietic agent. Proc. Natl. Acad. Sci. U.S.A. *102,* 7292-7296.

Barnes, D., and Sato, G. (1980). Methods for growth of cultured cells in serum-free medium. Anal. Biochem. *102,* 255-270.

Bevan, M. (1984). Binary *Agrobacterium* vectors for plant transformation. Nucleic Acids Res. *12,* 8711-8721.

Bezkorovainy, A., and Grohlich, D. (1970). Modification of carboxyl groups of transferrin. Biochim. Biophys. Acta. *214,* 37-43.

Boehm, R. (2007). Bioproduction of therapeutic proteins in the 21st century and the role of plants and plant cells as production platforms. Ann. N. Y. Acad. Sci. *1102,* 121-134.

Briere, N., Ferrari, J., and Chailler, P. (1991). Synergistic influence of epidermal growth factor, insulin and transferrin on human fetal kidney in culture. Biofactors *3,* 113-120.

Bullen, J.J. (1981). The significance of iron in infection. Rev. Infect. Dis. *3,* 1127-1138.

Bullen, J.J., Rogers, H.J., and Griffiths, E. (1978). Role of iron in bacterial infection. Curr. Top. Microbiol. Immunol. *80,* 1-35.

Byrne, S.L., Leverence, R., Klein, J.S., Giannetti, A.M., Smith, V.C., MacGillivray, R.T., Kaltashov, I.A., and Mason, A.B. (2006). Effect of glycosylation on the function of a soluble, recombinant form of the transferrin receptor. Biochemistry *45,* 6663-6673.

Carrington, J.C., and Freed, D.D. (1990). Cap-independent enhancement of translation by a plant potyvirus 5' nontranslated region. J. Virol. *64,* 1590-1597.

Daniell, H., Streatfield, S.J., and Wycoff, K. (2001). Medical molecular farming: production of antibodies, biopharmaceuticals and edible vaccines in plants. Trends Plant Sci. *6,* 219-226.

de Jong, G., van Dijk, J.P., and van Eijk, H.G. (1990). The biology of transferrin. Clin. Chim. Acta. *190,* 1-46.

de Smit, M.H., Hoefkens, P., de Jong, G., van Duin, J., van Knippenberg, P.H., and van Eijk, H.G. (1995). Optimized bacterial production of nonglycosylated human transferrin and its half-molecules. Int. J. Biochem. Cell Biol. *27,* 839-850.

Ellison, R.T. 3rd, Giehl, T.J., and LaForce, F.M. (1988). Damage of the outer membrane of enteric gram-negative bacteria by lactoferrin and transferrin. Infect. Immun. *56,* 2774-2781.

Fischer, R., Stoger, E., Schillberg, S., Christou, P., and Twyman, R.M. (2004). Plant-based production of biopharmaceuticals. Curr. Opin. Plant Biol. *7,* 152-158.

Friden, P.M., and Walus, L.R. (1993). Transport of proteins across the blood-brain barrier via the transferrin receptor. Adv. Exp. Med. Biol. *331,* 129-136.

Funk, W.D., MacGillivray, R.T., Mason, A.B., Brown, S.A., and Woodworth, R.C. (1990). Expression of the amino-terminal half-molecule of human serum transferrin in cultured cells and characterization of the recombinant protein. Biochemistry *29,* 1654-1660.

Furue, M.K., Na, J., Jackson, J.P., Okamoto, T., Jones, M., Baker, D., Hata, R., Moore, H.D., Sato, J.D., and Andrews, P.W. (2008). Heparin promotes the growth of human embryonic stem cells in a defined serum-free medium. Proc. Natl. Acad. Sci. U.S.A. *105,* 13409-13414.

Gallie, D.R., Tanguay, R.L., and Leathers, V. (1995). The tobacco etch viral 5' leader and poly(A) tail are functionally synergistic regulators of translation. Gene *165,* 233-238.

Gomme, P.T., McCann, K.B., and Bertolini, J. (2005). Transferrin: structure, function and potential therapeutic actions. Drug Discov. Today *10,* 267-273.

Harris, D.C., and Aisen, P. (1989). Physical biochemistry of the transferrins. In Iron Carriers and Iron Proteins, Loehr, T. M., Gray, H. N. and Lever, A. B. P. eds., Weinheim: VCH Publishers pp. 239-351.

Hoefkens, P., de Smit, M.H., de Jeu-Jaspars, N.M., Huijskes-Heins, M.I., de Jong, G., and van Eijk, H.G. (1996). Isolation, renaturation and partial characterization of recombinant human transferrin and its half molecules from *Escherichia coli.* Int. J. Biochem. Cell Biol. *28,* 975-982.

Holst, N., Bertheussen, K., Forsdahl, F., Hakonsen, M.B., Hansen, L.J., and Nielsen, H.I. (1990). Optimization and simplification of culture conditions in human *in vitro* fertilization (IVF) and preembryo replacement by serum-free media. J. In Vitro Fert. Embryo. Transf. *7,* 47-53.

Huebers, H.A., and Finch, C.A. (1987). The physiology of transferrin and transferrin receptors. Physiol. Rev. *67,* 520-582.

Hutchings, S.E., and Sato, G.H. (1978). Growth and maintenance of HeLa cells in serum-free medium supplemented with hormones. Proc. Natl. Acad. Sci. U.S.A. *75,* 901-904.

Iizuka, Y., and Murphy, M.J. Jr. (1986). Colony formation of granulocyte (CFU-g) and macrophage (CFU-m) precursors in serum- and albumin-free culture: effect of transferrin on clonal growth. Exp. Cell Biol. *54,* 275-280.

Ikeda, R.A., Bowman, B.H., Yang, F., and Lokey, L.K. (1992). Production of human serum transferrin in *Escherichia coli.* Gene *117,* 265-269.

Keenan, J., Pearson, D., O'Driscoll, L., Gammell, P., and Clynes, M. (2006). Evaluation of recombinant human transferrin (DeltaFerrin(TM)) as an iron chelator in serum-free media for mammalian cell culture. Cytotechnology *51,* 29-37.

Lerouge, P., Cabanes-Macheteau, M., Rayon, C., Fischette-Laine, A.C., Gomord, V., and Faye, L. (1998). N-glycoprotein biosynthesis in plants: recent developments and future trends. Plant Mol. Biol. *38,* 31-48.

Li, H., and Qian, Z.M. (2002). Transferrin/transferrin receptor-mediated drug delivery. Med. Res. Rev. *22,* 225-250.

Lienard, D., Sourrouille, C., Gomord, V., and Faye, L. (2007). Pharming and transgenic plants. Biotechnol. Annu. Rev. *13,* 115-147.

Lim, H.J., Kim, Y.K., Hwang, D.S., and Cha, H.J. (2004). Expression of functional human transferrin in stably transfected *Drosophila* S2 cells. Biotechnol. Prog. *20,* 1192-1197.

Liu, Y., Tao, J., Li, Y., Yang, J., Yu, Y., Wang, M., Xu, X., Huang, C., Huang, W., Dong, J., Li, L., Liu, J., Shen, G., and Tu, Y. (2009). Targeting hypoxia-inducible factor-1alpha with Tf-PEI-shRNA complex via transferrin receptor-mediated endocytosis inhibits melanoma growth. Mol. Ther. *17,* 269-277.

Ma, S., Huang, Y., Davis, A., Yin, Z., Mi, Q., Menassa, R., Brandle, J.E., and Jevnikar, A. (2005). Production of biologically active human interleukin-4 in transgenic tobacco and potato. Plant Biotech. J. *3,* 309-318.

MacGillivray, R.T., Mendez, E., Shewale, J.G., Sinha, S.K., Lineback-Zins, J., and Brew, K. (1983). The primary structure of human serum transferrin. The structures of seven cyanogen bromide fragments and the assembly of the complete structure. J. Biol. Chem. *258,* 3543-3553.

MacGillivray, R.T., Moore, S.A., Chen, J., Anderson, B.F., Baker, H., Luo, Y., Bewley, M., Smith, C.A., Murphy, M.E., Wang, Y., Mason, A.B., Woodworth, R.C., Brayer, G.D., and Baker, E.N. (1998). Two high-resolution crystal structures of the recombinant N-lobe of human transferrin reveal a structural change implicated in iron release. Biochemistry *37,* 7919-7928.

Mason, A.B., Funk, W.D., MacGillivray, R.T., and Woodworth, R.C. (1991). Efficient production and isolation of recombinant amino-terminal half-molecule of human serum transferrin from baby hamster kidney cells. Protein Expr. Purif. *2,* 214-220.

Mason, A.B., Halbrooks, P.J., Larouche, J.R., Briggs, S.K., Moffett, M.L., Ramsey, J.E., Connolly, S.A., Smith, V.C., and MacGillivray, R.T. (2004). Expression, purification, and characterization of authentic monoferric and apo-human serum transferrins. Protein Expr. Purif. *36,* 318-326.

Mason, A.B., He, Q.Y., Adams, T.E., Gumerov, D.R., Kaltashov, I.A., Nguyen, V., and MacGillivray, R.T. (2001). Expression, purification, and characterization of recombinant nonglycosylated human serum transferrin containing a C-terminal hexahistidine tag. Protein Expr. Purif. *23,* 142-150.

Mason, A.B., Miller, M.K., Funk, W.D., Banfield, D.K., Savage, K.J., Oliver, R.W., Green, B.N., MacGillivray, R.T., and Woodworth, R.C. (1993a). Expression of glycosylated and nonglycosylated human transferrin in mammalian cells. Characterization of the recombinant proteins with comparison to three commercially available transferrins. Biochemistry *32,* 5472-5479.

Mason, A.B., Woodworth, R.C., Oliver, R.W., Green, B.N., Lin, L.N., Brandts, J.F., Tam, B.M., Maxwell, A., and MacGillivray, R.T. (1996). Production and isolation of the recombinant N-lobe of human serum transferrin from the methylotrophic yeast *Pichia pastoris*. Protein Expr. Purif. *8,* 119-125.

Menassa, R., Du, C., Yin, Z.Q., Ma, S., Poussier, P., Brandle, J., and Jevnikar, A.M. (2007). Therapeutic effectiveness of orally administered transgenic low-alkaloid tobacco expressing human interleukin-10 in a mouse model of colitis. Plant Biotechnol. J. *5,* 50-59.

Mitra, A., and Zhang, Z. (1994). Expression of a human lactoferrin cDNA in tobacco cells produces antibacterial protein(s). Plant Physiol. *106,* 977-981.

Nakase, I., Lai, H., Singh, N.P., and Sasaki, T. (2008). Anticancer properties of artemisinin derivatives and their targeted delivery by transferrin conjugation. Int. J. Pharm. *354,* 28-33.

Moore, D.G., Yancey, R.J., Lankford, C.E., and Earhart, C.F. (1980). Bacteriostatic enterochelin-specific immunoglobulin from normal human serum. Infect. Immun. *27,* 418-423.

Osborn, M.J., McElmurry, R.T., Peacock, B., Tolar, J., and Blazar, B.R. (2008). Targeting of the CNS in MPS-IH using a nonviral transferrin-alpha-L-iduronidase fusion gene product. Mol. Ther. *16,* 1459-1466.

Salamah, A.A., and Al-Obaidi, A.S. (1995). Effect of some physical and chemical factors on the bactericidal activity of human lactoferrin and transferrin against *Yersinia pseudotuberculosis*. New Microbiol. *18,* 275-281.

Sargent, P.J., Farnaud, S., Cammack, R., Zoller, H.M., and Evans, R.W. (2006). Characterisation of recombinant unglycosylated human serum transferrin purified from *Saccharomyces cerevisiae*. Biometals *19,* 513-519.

Steinlein, L.M., and Ikeda, R.A. (1993). Production of N-terminal and C-terminal human serum transferrin in *Escherichia coli*. Enzyme Microb. Technol. *15,* 193-199.

Takase, K., Hagiwara, K., Onodera, H., Nishizawa, Y., Ugaki, M., Omura, T., Numata, S., Akutsu, K., Kumura, H., and Shimazaki, K. (2005). Constitutive expression of human lactoferrin and its N-lobe in rice plants to confer disease resistance. Biochem. Cell Biol. *83,* 239-249.

Wang, D.J., Brandsma, M., Yin, Z., Wang, A., Jevnikar, A.M., and Ma, S. (2008). A novel platform for biologically active recombinant human interleukin-13 production. Plant Biotechnol. J. *6,* 504-515.

Watkins, L.F., Lewis, L.R., and Levine, A.E. (1990). Characterization of the synergistic effect of insulin and transferrin and the regulation of their receptors on a human colon carcinoma cell line. Int. J. Cancer *45,* 372-375.

Widera, A., Bai, Y., and Shen, W.C. (2004). The transepithelial transport of a G-CSF-transferrin conjugate in Caco-2 cells and its myelopoietic effect in BDF1 mice. Pharm. Res. *21,* 278-284.

Widera, A., Kim, K.J., Crandall, E.D., and Shen, W.C. (2003). Transcytosis of GCSF-transferrin across rat alveolar epithelial cell monolayers. Pharm. Res. *20,* 1231-1238.

Yet, M.G., and Wold, F. (1990). The distribution of glycan structures in individual N-glycosylation sites in animal and plant glycoproteins. Arch. Biochem. Biophys. *278,* 356-364.

Chapter 4
General Conclusion

4.1 Research findings

The primary goal of this research thesis was to investigate a novel strategy to reduce production and therapeutic administration limitations of therapeutic GLP-1 with the intent of furthering the transition to an effective therapy against Type II diabetes. To achieve this goal, two major objectives have been addressed: (1) the accumulation of biologically active synthetic rGLP-1 decamer in transformed tobacco plants intended as a novel source for GLP-1 and (2), the accumulation of biologically functioning rhsTf in transformed tobacco plants intended to establish a framework for future possible genetic fusions to GLP-1 for enhanced therapeutic GLP-1 bioavailability upon oral administration.

The first objective of this thesis was to demonstrate the feasibility of rGLP-1 accumulation in transgenic tobacco plants. As the GLP-1 peptide is quite small in molecular mass (~3.4 kDa), the GLP-1 protein was expressed in transgenic tobacco plants as a multimer repeat protein consisting of ten consecutive repeats of *GLP-1* monomer. This GLP-1 decamer strategy was intended to enhance rGLP-1 stability and allow for subsequent recombinant protein accumulation. To initiate this study, a binary plant expression vector was generated for constitutive expression of the synthetic *GLP-1* decamer, designated pALP-GLP-1x10. The transgenic tobacco cultivar 81V9 was stably

transformed with pALP-GLP-1x10 by *Agrobacterium*-mediated nuclear gene transfer. The presence of the *GLP-1x10* transgene and recombinant transcript was confirmed by PCR and RT-PCR respectively. Immunoblot analysis using anti-GLP-1 antibody detected a single band of appropriate molecular mass (~36 kDa) corresponding in size to that of recombinant GLP-1 decamer in TSP extracted from tobacco plants transformed with pALP-GLP-1x10. No bands were detected with immunoblotting under identical conditions using untransformed 81V9 tobacco control. Biological activity of the plant-derived rGLP-1 decamer was confirmed by the ability to stimulate insulin secretion *in vitro* from a mouse pancreatic beta-cell line (MIN6). Not only can plant-derived GLP-1 decamer significantly stimulate insulin secretion from MIN6 cells *in vitro*, but also the stimulatory effect was most likely the result of the synthetic rGLP-1 decamer and not the breakdown of the rGLP-1 decamer to its native GLP-1 monomer constituents. This thesis is the first study to demonstrate the viable accumulation of rGLP-1 as a decamer protein in transgenic tobacco. Furthermore, this thesis is the first study to present findings of GLP-1 insulin stimulatory effects *in vitro* when GLP-1 is retained as a synthetic decamer and not in its native GLP-1 monomer configuration.

The second objective of this thesis was to determine if hsTf could be expressed and accumulated in transgenic tobacco. For this aim, a binary plant expression vector intended for constitutive expression of *hsTf* was generated and designated pRJC-hsTf. The transgenic tobacco cultivar 81V9 was stably transformed with pRJC-hsTf by *Agrobacterium*-mediated nuclear gene transfer. The presence of *hsTf* transgene and recombinant transcript was confirmed by PCR and RT-PCR respectively. Immunoblot analysis using anti-hsTf antibody detected a single band of approximate molecular mass

(~76 kDa) corresponding in size to that of rhsTf from TSP extracts derived from tobacco plants transformed with pRJC-hsTf. No bands were detected with immunoblotting under identical conditions with untransformed 81V9 tobacco control. The biological function of plant-derived rhsTf was assessed by its ability to bind iron reversibly *in vitro*. Measurements of A_{465} / A_{280} indicate that plant-derived rhsTf retains similar iron binding properties to an hsTf standard. Potential commercial applications of plant-derived rhsTf were assessed by analysis of plant-derived rhsTf to affect bacterial growth negatively *in vitro*. Results here indicate that plant-derived rhsTf significantly delays growth of *P. syringae* compared to negative controls *in vitro*. The ability of plant-derived rhsTf to stimulate mammalian cell growth *in vitro* was also assessed. Plant-derived rhsTf can stimulate mammalian HeLa cell growth *in vitro* over a 4-day period and is capable of physically interacting with HeLa cells *in vitro*. Taken together, results demonstrated here indicate that plant-derived rhsTf retains many of its native functions, greatly enhancing its potential commercial and therapeutic application.

4.2 Anticipated significance

An efficient method for the production of biologically active rGLP-1 for the treatment of symptoms associated with Type II diabetes has yet to be demonstrated. Previous research demonstrated that GLP-1 could be accumulated in transgenic rice, either fused to a chaperone protein or expressed as a pentamer repeat of itself (Sugita *et al.*, 2005; Yasuda *et al.*, 2006). In all reported cases, rGLP-1 must be enzymatically cleaved from its stabilizing chaperone *in vitro* before biological activation can be determined. Furthermore, a rice-derived GLP-1 pentamer had no reported biological

activity (Yasuda *et al.*, 2006). This thesis presents the first findings that the plant bioreactor permits viable accumulation of a synthetic rGLP-1 decamer. More importantly, this thesis is the first to suggest that a synthetic GLP-1 decamer indeed contains an insulin-stimulatory effect *in vitro*, previously only shown with the native GLP-1 monomer. The synthetic GLP-1 decamer activity has great potential to reduce rGLP-1 production costs in a commercial scheme. As a result, the novel production platform should offer a new alternative source for biologically active rGLP-1, in hopes of providing a viable solution for the treatment of symptoms associated with Type II diabetes.

If rGLP-1 is to be made available as a future therapy against Type II diabetes, the development of a novel GLP-1 administration technique, other than subcutaneous injection, may alleviate concerns often associated with injection and help increase patient compliance. Oral administration of GLP-1 for Type II diabetes therapy has been proposed, although a scheme to facilitate transport of orally administered GLP-1 across the GI tract and into systemic circulation, where it can elicit its therapeutic effect, has yet to be demonstrated. Therapeutic genetic fusions to hsTf have shown the ability of hsTf to transport therapeutic proteins of choice out of the GI tract and into systemic circulation following oral administration (Li and Qian, 2002; Shah and Shen, 1996; Widera *et al.*, 2004). For GLP-1 fusion to hsTf in transgenic plants to be assessed for enhanced GLP-1 bioavailability following oral administration, hsTf accumulation within the plant bioreactor must first be demonstrated. This thesis presents the first findings of rhsTf being transformed and accumulating in any plant host. Furthermore, plant-derived rhsTf retains an ability to reversibly bind iron *in vitro*. By itself, this thesis demonstrates two

novel applications for plant-derived rhsTf, namely the ability to stimulate mammalian cell growth and the ability to delay pathogenic bacterial growth *in vitro*. More importantly, viable plant-derived rhsTf production establishes the framework needed to justify future genetic fusions of GLP-1 to hsTf in the plant bioreactor for the intent of enhancing bioavailability of GLP-1 upon oral administration.

The results from this thesis indicate a number of future avenues of research for treatment against symptoms associated with Type II diabetes. Future investigation is hoped to assess the potential of plant-derived GLP-1 decamer to reduce symptoms associated with Type II diabetes *in vivo*. Work towards fusing GLP-1 to hsTf and accumulating the fusion protein *in planta* is also foreseen as the next logical step. To provide further insight, the comparison of therapeutic potency of a plant-derived GLP-1 decamer and a GLP-1 decamer fused to hsTf delivered orally to an *in vivo* animal model for Type II diabetes should be attempted. In addition, pathogenic protection conferred by *in vivo* accumulation of rhsTf in transgenic plants could also be assessed as a new method for crop disease resistance.

4.3 References

Li, H., and Qian, Z.M. (2002). Transferrin/transferrin receptor-mediated drug delivery. Med. Res. Rev. *22,* 225-250.

Shah, D., and Shen, W.C. (1996). Transcellular delivery of an insulin-transferrin conjugate in enterocyte-like Caco-2 cells. J. Pharm. Sci. *85,* 1306-1311.

Sugita, K., Endo-Kasahara, S., Tada, Y., Lijun, Y., Yasuda, H., Hayashi, Y., Jomori, T., Ebinuma, H., and Takaiwa, F. (2005). Genetically modified rice seeds accumulating GLP-1 analogue stimulate insulin secretion from a mouse pancreatic beta-cell line. FEBS Lett. *579,* 1085-1088.

Widera, A., Bai, Y., and Shen, W.C. (2004). The transepithelial transport of a G-CSF-transferrin conjugate in Caco-2 cells and its myelopoietic effect in BDF1 mice. Pharm. Res. *21,* 278-284.

Yasuda, H., Hayashi, Y., Jomori, T., and Takaiwa, F. (2006). The correlation between expression and localization of a foreign gene product in rice endosperm. Plant Cell Physiol. *47,* 756-763.

Appendix 1

Supplementary Materials and Methods

1.1 Bacterial strains

For all experiments within this thesis describing the manipulation of plasmid DNA (pDNA), DH5α *E. coli* cells (Invitrogen) were used as a host. DH5α cells were maintained on Luria-Bertani (LB) medium [1% tryptone, 0.5% (w/v) yeast extract, 1% (w/v) NaCl] containing 1.5% (w/v) agar and selective antibiotics at 37°C. DH5α liquid cultures used for pDNA extraction were grown in Terrific Broth (TB) medium [1.2% (w/v) tryptone, 2.4% (w/v) yeast extract, 0.4% (w/v) glycerol, 17 mM KH_2PO_4, 72 mM K_2HPO_4] shaking at 250 rpm at 37°C. *A. tumefaciens* strain LBA4404 was used in all described *Agrobacterium*-mediated plant transformation experiments. LBA4404 was maintained on Tryptone/yeast extract/calcium chloride (TYC) medium [1% (w/v) tryptone, 0.5% (w/v) yeast extract, 0.066% (w/v) $CaCl_2$] containing 1.5% (w/v) agar and rifampicin (25 mg/mL) at 28°C. For liquid cultures, LBA4404 was grown in TYC broth containing rifampicin (25 mg/mL) lacking agar, shaking at 250 rpm at 28°C. For the rhsTf prokaryote growth assay, *P. syringae* was maintained in liquid LB media shaking at 250 rpm at 28°C containing no antibiotics.

Antibiotic concentrations in growth media used for selection was as follows: transformed DH5α *E. coli* cells were selected for by resistance to carbenicillin

(100 μg/mL) or kanamycin (50 μg/mL); transformed *A. tumefaciens* was selected for by resistance to kanamycin (50 μg/mL) and rifampicin (25 μg/mL).

1.2 Rapid alkaline lysis mini-prep of pDNA

To extract pDNA from transformed DH5α cells, the rapid alkaline lysis mini-prep method was used (Birnboim and Dolly, 1979). Transformed DH5α cells derived from a single colony were used to inoculate 3 mL of TB liquid medium containing appropriate antibiotic. DH5α cells were grown overnight at 37°C, shaking at 250 rpm. All described centrifugations were performed on a Sigma-Aldrich 1-15 centrifuge. A total of 1.5 mL of overnight grown transformed DH5α culture was transferred into a 1.5 mL Eppendorf tube and centrifuged for 30 s at 12,000-x G. After discarding the supernatant, the cell pellet was resuspended in 100 μL of Glucose/Tris/EDTA (GTE) buffer [50 mM glucose, 25 mM Tris-HCl, 10 mM EDTA, pH 8.0] and incubated at room temperature for 5 min. Following incubation, 200 μL of NaOH/SDS [0.2 M NaOH, 1% (w/v) SDS] was added, gently mixed by inversion, and the mixture was incubated on ice for 5 min. Following incubation, 150 μL of potassium acetate [29.5% (v/v) glacial acetic acid, adjusted to pH 4.8 using 5 M KOH] was added and mixed by vortexing for 2 s followed by a 5 min incubation on ice. The mixture was centrifuged at 12,000-x G for 5 min and the supernatant was collected, mixed with 600 μL of isopropanol and allowed to incubate at room temperature for 5 min. To pellet the insoluble pDNA, the mixture was centrifuged at 12,000-x G for 5 min, followed by a subsequent wash with 1 mL of 70% (v/v) ethanol. The resulting pDNA pellet was vacuum dried and dissolved in 50 μL double distilled water (ddH_20) and 1 μL RNase (Fermentas).

1.3 Polymerase chain reaction (PCR)

PCR was used in this thesis for manipulation of DNA to incorporate novel restriction sites as well as for screening of putative transformant tobacco gDNA for the presence of transgene. In brief, approximately 50-100 ng of template DNA was used for a 50 μL PCR reaction. Each reaction mixture contained 1X PCR buffer, 2 M dNTPs, 1 μM of both forward and reverse primers, 2.5 mM $MgCl_2$ and 1 unit of DNA polymerase. All PCR reactions used high fidelity *pfu* DNA polymerase (Fermentas) except for PCR reactions utilized for screening, where Taq DNA polymerase (Fermentas) was used instead. PCR products were purified with the QIAquick gel extraction kit (Qiagen, Mississauga, ON) after size separation by electrophoresis on a 0.75% (w/v) agarose gel.

1.4 DNA ligations

All DNA ligations used the Rapid Ligation Kit (Fermentas). A reaction mixture containing ~3 μg of DNA insert, 1 μg of backbone pDNA, 4 μL of 5X reaction buffer, and 1 μL of T4 DNA ligase, was adjusted to 20 μL with ddH_2O. Following a 15 min incubation at room temperature, 5 μL of the ligation mixture was transformed into chemically competent DH5α cells (Invitrogen) by heat shock. For electroporation, 3 μL of the ligation mixture was transformed into electrocompetent DH5α cells.

1.5 *E. coli* transformation

Heat shock transformation was achieved using chemical competent DH5α cells transformed with pDNA. Only bacterial transformations involving *GLP-1* used heat

Table 2. Primers used for PCR and RT-PCR reactions

Primer Name	Nucleotide Sequence	Purpose
P1	5' AATT**CCATGG**GGC ATTCTGAGGGAACCTTCACCTCTGACG 3'	Cloning
P2	5' AATTGAATTCAATTCTCGAGCCTTCCCTTCACCACCAAGC 3'	Cloning
P3	5' AATT**GTCGAC**CATTCTGAGGGAACCTTCACCTCTGACG 3'	Cloning / Screening
P4	5' AATTCTCGAG**TTA**ATGATGATGATGATGATGCCTTCCCTTCACCAACCAAGC 3'	Cloning / Screening
P5	5' CGAATCTCAAGCAATCAAGC 3'	Screening
TF1	5' ATGATATC**ATG**AGGCTCGCCGTGGGAGC 3'	Cloning / Screening
TF2	5' AA**TCTAGA**TTA*AAGCTCATCCTT*ATGATGATGATGATGATGAGGTCTACGGAAAGTGCAGGC 3'	Cloning / Screening
Actin-F	5' CAGCAACTGGGACGATATGG 3'	RT-PCR control
Actin-R	5' ATTTCCCGTTCAGCACTAGTGG 3'	RT-PCR control

Note: All primers used in this thesis are listed in Table 1. Additional information about primers are as follows: (P1) bold – *Nco*I restriction site. (P2) double underline – *Xho*I restriction site. (P3) bold – *Sal*I restriction site. (P4) underline – *Xho*I restriction site, bold – stop codon, double underline – 6xHis tag. (TF1) underline, *Eco*RV restriction site, bold – start codon. (TF2) bold – *Xba*I restriction site, double underline – stop codon, italic – KDEL retention signal, underline – 6xHis tag.

shock due to sequence length. Approximately 50 ng of pDNA was added to 40 μL of competent DH5α cells (Invitrogen), gently mixed and placed on ice for 35 min. Cells were then heat shocked in a 37°C water bath for 5 min and cooled on ice for 10 min. Following transformation, cells were transferred to 800 μL of SOC media [0.5% (w/v) yeast extract, 2% (w/v) tryptone, 10 mM NaCl, 2.5 mM KCl, 10 mM $MgCl_2$, 10 mM $MgSO_4$, 20 mM glucose] and grown for 1 h at 37°C, shaking at 250 rpm. Following incubation, 200 μL of resulting culture was spread on LB agar plates containing appropriate antibiotics for selection.

Electrocompetent DH5α cells were transformed with pDNA by electroporation (Miller and Nickoloff, 1995). Only bacterial transformations involving *hsTf* used electroporation due to sequence length. In brief, 3 μL of ligation mixture was added to 40 μL of electrocompetent cells and incubated on ice for 5 min. The cell mixture was added to cold 1 mm electroporation cuvettes (Bio-Rad Laboratories) and placed in the chamber slide of a MicroPulser™ electroporation apparatus (Bio-Rad Laboratories). The cell mixture was pulsed once at 1.8 kV and immediately added to 1 mL of SOC and gently resuspended. The resulting cell suspension was incubated at 37°C for 1 h, shaking at 250 rpm. Following incubation, 50 μL of the resulting culture was spread on LB plates containing appropriate antibiotics for selection.

1.6 *A. tumefaciens* transformation

A. tumefaciens strain LBA4404 was transformed by tri-parental mating (Wise *et al.*, 2006). Transformation was performed using DH5α containing plant expression vector pDNA, DH5α containing helper plasmid pRK2013 (Bio-Rad Laboratories) and

LBA4404 (provided by the Ma laboratory) plated together on TYC agar plates. The three cell types were incubated overnight at 28°C and a streak of the cell mixture was subsequently inoculated in 1 mL of LB liquid media and grown for 1 h at 28°C shaking at 250 rpm. A 30 µl aliquot of this mixture was plated on TYC agar containing kanamycin (50 µg/mL) and rifampicin (25 µg/mL). After 48 h incubation at 28°C, single colonies were transferred into 1 mL of TYC liquid media containing kanamycin (50 µg/mL) and rifampicin (25 µg/mL) and grown overnight at 28°C, shaking at 250 rpm. The resulting LBA4404 culture was used for stable tobacco leaf-disc transformation. Unconjugated DH5α and LBA4404 were plated separately on TYC containing rifampicin and kanamycin as a negative control.

1.7 Stable tobacco transformation

Low-alkaloid *N. tabacum* cv 81V9 was transformed by leaf disc co-cultivation with LBA4404 containing the desired plant expression vector (Horsch *et al.*, 1985). LBA4404 cells were pelleted and resuspended in MSO liquid media [Murashige and Skoog salts, 3% (w/v) sucrose]. Sterile tobacco leaf-discs were cut into 0.5 cm^2 segments and floated in 10 mL MSO liquid media containing transformed LBA4404. Leaf-discs were incubated for 48 h at 25°C in a growth chamber on a 16 h daylight cycle with light intensity of approximately 150 µM photons $m^{-2}s^{-1}$. Following incubation, leaf-discs were washed with MSO liquid media, blotted dry and transferred to MS104 callus inducing media [Murashige and Skoog salts, 3% (w/v) sucrose, 10 mg/L benzylaminopurine (BA), 0.1 mg/L naphthalene acetic acid (NA), 0.8% (w/v) phytagar] containing carbenicillin (500 µg/mL) and kanamycin (100 µg/mL). Leaf discs were grown under previously

described growth chamber conditions and transferred to new plates every two weeks. After several rounds of transfer, callus induction was observed followed by shoot growth. Shoots growing from calli were isolated and transferred to Magenta boxes containing MS shoot inducing media [Murashige and Skoog salts, 3% (w/v) sucrose, 1.0 mg/L BA, 0.1 mg/L NA, 0.8% (w/v) phytagar] containing carbenicillin (50 μg/mL) and kanamycin (50 μg/mL). As plantlets matured, they were transferred into a greenhouse and maintained for subsequent screening.

1.8 Tobacco gDNA extraction

A basic phenol/chloroform method for DNA extraction was used to extract gDNA from tobacco plants. Tobacco leaf tissue approximately 2 cm in diameter was homogenized in extraction buffer [0.2 M Tris-HCl (pH 7.5), 0.25 M NaCl, 25 mM EDTA, 0.5% (w/v) SDS] and incubated at room temperature for 1 h. Samples were centrifuged at 12,000-x G for 10 min and the supernatant collected. To the mixture, sodium acetate [3 M CH_3COONa, pH 4.8] and phenol/chloroform (1:1 (v/v)) were added and the whole mixture vortexed for 10 s followed by centrifugation at 12,000-x G for 5 min. Following centrifugation, the aqueous phase was collected, added to 300 μL of isopropanol, mixed by inversion and incubated at room temperature for 2 min. The solution was then pelleted by centrifugation at 12,000-x G for 10 min and washed with 70% (v/v) ethanol. The final DNA pellet was dried at 37°C for 10 min and resuspended in 50 μL of ddH_2O for further analysis.

1.9 Statistical Analysis

All statistics reported in this thesis used a paired two-tailed Student's *t*-test to determine whether or not differences between samples were significant. Values of $p<0.05$ were held to be significant.

Appendix 1 References

Birnboim, H. C., and Doly, J. (1979). A rapid alkaline extraction procedure for screening recombinant plasmid DNA. Nucleic Acids Research *7*, 1513-1523.

Horsch R.B., Fry J.E., Hoffmann N.L., Eicholtz D., Rogers S.G., and Fraley R.T. (1985). A simple and general method for transferring genes into plants. Science *227,* 1229-1231.

Miller, E.M., & Nickoloff, J.A. (1995). *Escherichia coli* electrotransformation. Methods Mol. Biol. *47*, 105-113.

Wise, A.A., Liu, Z., and Binns, A.N. (2006). Three methods for the introduction of foreign DNA into *Agrobacterium*. Methods Mol. Biol. *343,* 43-53.